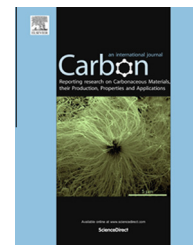


Available at www.sciencedirect.com

ScienceDirect

journal homepage: www.elsevier.com/locate/carbon

Printing nanostructured carbon for energy storage and conversion applications



Stephen Lawes, Adam Riese, Qian Sun, Niancai Cheng, Xueliang Sun *

Department of Mechanical and Materials Engineering, University of Western Ontario, London, ON N6A 3K7, Canada

ARTICLE INFO

Article history:

Received 16 January 2015

Accepted 4 April 2015

Available online 8 April 2015

ABSTRACT

Printing is rapidly emerging as a novel fabrication technique for energy storage and conversion technologies. As nanostructured carbons replace traditional materials in energy devices due to their unique structures and properties, intensive research efforts have focused on developing methods to print these new materials. Inkjet printing, screen printing, transfer printing, and 3D printing are increasingly used to print carbon nanomaterials. After a brief introduction of the basic operating principles of each of these techniques, methods for printing fullerenes, graphene, carbon nanotubes, carbon black, and activated carbon are reviewed. Subsequently, the applications of printing techniques for fabricating batteries, supercapacitors, fuel cells, and solar cells are discussed, followed by a perspective on the current challenges and future outlook of printing nanostructured carbon materials for these devices.

© 2015 Elsevier Ltd. All rights reserved.

1. Introduction

Printing techniques have existed in a variety of forms for millennia. The invention of the printing press was one of the most significant advances in history and it transformed the way information was distributed, having widespread social implications. Since then, many printing techniques have been developed, enabling faster throughput and higher quality prints on a multitude of different substrates. Some of these techniques include screen printing, lithography, inkjet printing, transfer printing, and recently, 3D printing.

The most common use of printing is the reproduction of text with ink on paper, however recently there has been a noteworthy rise in the development of printable functional materials. Most printing inks have evolved considerably since the earliest printing, and the blossoming of nanotechnology in recent decades has brought with it an opportunity for

further advancements. Similarly, computers and controlled machinery mean super-fast and precise printing is available at low costs. Now techniques exist for printing nanoparticle dispersions, conductive polymers, biological molecules, and nanostructured carbons. Using these techniques, printing has become much more than the transfer of words onto pages. Functional printing technology has been used to fabricate displays, biological tissue scaffolds, battery electrodes, supercapacitors, fuel cell catalysts, and solar cells.

Carbon exists in many forms including nanostructures such as graphene, carbon nanotubes (CNTs), and fullerenes, which are some of the most fervently and widely studied nanomaterials today. These three materials are similar in their atomic bonding structure, comprised of sp^2 bonded carbon, but are manifest as sheets, tubes, and spheres in 2, 1, and 0 dimensions, respectively. Both graphene and CNTs exhibit highly attractive properties such as good thermal

* Corresponding author.

E-mail address: xsun@eng.uwo.ca (X. Sun).

<http://dx.doi.org/10.1016/j.carbon.2015.04.008>

0008-6223/© 2015 Elsevier Ltd. All rights reserved.

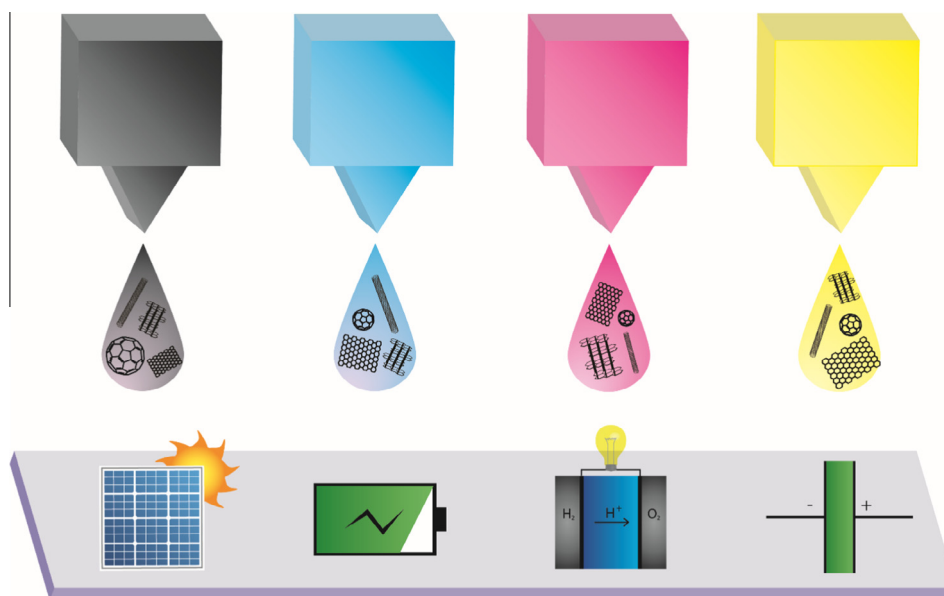


Fig. 1 – Schematic representing the printing process of nanostructured carbon materials for solar cells, batteries, fuel cells, and supercapacitors. (A color version of this figure can be viewed online.)

and electrical conductivity, mechanical strength, and chemical stability. Fullerenes also possess unique optical and electronic properties, especially when functionalized. As a result, nanostructured carbons are being used in a growing number of established and emerging applications. Printing these materials has been recognized as an excellent approach for preparing functional structures and films with precise thickness control, patternability, and minimal wasted material.

Here we review printing of carbon nanomaterials and the application of printed carbons for energy storage and conversion (Fig. 1). This review begins with an introduction of basic printing methods and principles, highlighting and comparing several of the most important techniques. Subsequently, a detailed review of printed carbon nanomaterials is given. Essential parameters for printing these materials such as functionalization, surface treatment, and ink preparation will be discussed with specific examples from the literature given throughout. Finally, applications of printed carbon nanomaterials for energy storage and conversion are discussed, followed by an outlook on potential future trends in printing nanostructured carbon research and technology.

2. Principles of printing technologies

The fundamental principles of four major printing techniques are introduced here. Inkjet printing, screen printing, and transfer printing are all commonly used techniques for depositing nanostructured carbon onto substrates of varying size, surface energy, and flexibility for energy applications. 3D printing, on the other hand is an emerging technology, with very few studies of its use for carbon nanomaterials reported. However, it is becoming a popular technique in both academic research and industry, and is therefore discussed briefly in this section.

2.1. Inkjet printing

Inkjet printing is an additive technique for patterning two-dimensional structures onto a substrate. It precisely deposits ink droplets at desired locations without pre-patterning the substrate, making it simple to use while minimizing wasted material. It has been widely adopted in industry as a rapid fabrication technique, ranging from advertising to material tagging to printed circuit boards.

Inkjet printing has also been successfully applied to fabricating energy storage and conversion devices, such as battery electrodes [1–6], supercapacitors [7–11], and solar cells [12–16]. It can be used to fabricate thin films or patterns of uniform thickness, which can be controlled by the number of layers printed on top of one another. Inkjet printing technology has many advantages over other fabrication techniques, including cost-effectiveness, ease of use, minimal wasted material, scalability, and the ability to deposit designed patterns.

Principally, inkjet printing can be divided into continuous inkjet (CIJ) and drop-on-demand (DOD) methods. CIJ printing involves pumping liquid ink through a nozzle where a continuous stream of droplets is formed by a vibrating piezoelectric crystal. Some droplets are charged by passing them through an electric field, which can be varied to control the degree of charging. The droplets then pass through another electric field, with the more highly charged droplets deflecting more than those with a lesser charge. In this way an image can be produced, with unused ink being collected in a gutter and recycled. On the other hand, DOD printers eject material only when required. This involves forcing ink out of a series of nozzles mounted on a print head. Because DOD printers do not recycle ink, which may result in degradation upon exposure to atmosphere, they are the standard choice for printing functional materials including graphene and carbon

nanotubes. In addition, DOD printing generally wastes less material; it is therefore a more suitable technique for printing expensive materials.

The three main stages of inkjet printing are illustrated in Fig. 3a: droplet ejection, droplet spreading, and droplet solidification. The print head is first moved to the desired position, where droplets are ejected through the nozzle and travel to the substrate. Upon impact, they spread along the surface and join with other droplets, forming a thin film of liquid ink. Finally, the solvent evaporates, leaving the solid contents of the ink remaining on the substrate.

To achieve droplet ejection in DOD printers, there are two main types of inkjet print heads: thermal and piezoelectric. Thermal print heads contain a resistor inside the ink chamber which, upon an applied voltage, will superheat the ink above the bubble nucleation temperature. The bubble expands, forcing ink out of the chamber and through the nozzle. Once the ink is ejected, the chamber rapidly cools, allowing more ink to refill the chamber. This entire process occurs within a few microseconds [17]. Piezoelectric inkjet print heads, on the other hand, contain a piezoelectric element that pulsates upon electrical excitation, which forms a pressure wave that forces ink out of the chamber. The vibration of the piezoelectric material can be precisely tuned to control droplet ejection from the nozzle. Typically, inkjet print heads comprise of hundreds of ink chambers and nozzles to achieve high throughput. A higher number of nozzles allows for printing of higher resolution patterns in shorter time frames, an important metric for large-scale production.

Thermal print heads are generally cheaper and require less maintenance than piezoelectric print heads because they contain no moving parts. The cartridge on which the print heads are mounted can simply be replaced by the user for relatively low cost if the nozzles become clogged or broken. Piezoelectric print heads, however, typically require more expensive maintenance procedures by a technician if their piezoelectric crystals become damaged. On the other hand, piezoelectric print heads are preferable for printing a wide range of functional materials since they do not require any heating of the ink, which can result in degradation of the active materials. In addition, a wider range of solvents can be used with the piezoelectric systems, including water, oils, and organic solvents; thermal print heads are generally limited to aqueous inks due to the nucleation temperature required for droplet ejection. Also, the viscosity, surface tension, and density of the ink must be more precisely controlled when using thermal print heads. Typically the ink viscosity must be approximately 10 cP [18]. Therefore, piezoelectric print heads are more commonly used for inkjet printing of carbon nanomaterials due to their versatility in terms of the ink's composition and physical properties.

For both types of print head, droplet ejection is dependent on the viscosity, surface tension, and density of the ink, the shape and size of the nozzle, and the ejection velocity of the droplet. These parameters are described by the Reynolds (Re), Weber (We), and Ohnesorge (Oh) numbers. As shown in Fig. 2a, there is a region in which Re, We, and Oh are optimized for ideal jetting. In the figure, Z is defined as the reciprocal of the Ohnesorge number, $1/Oh$. Generally, high Z fluids (high viscosity, low surface tension) will be unable to form droplets that

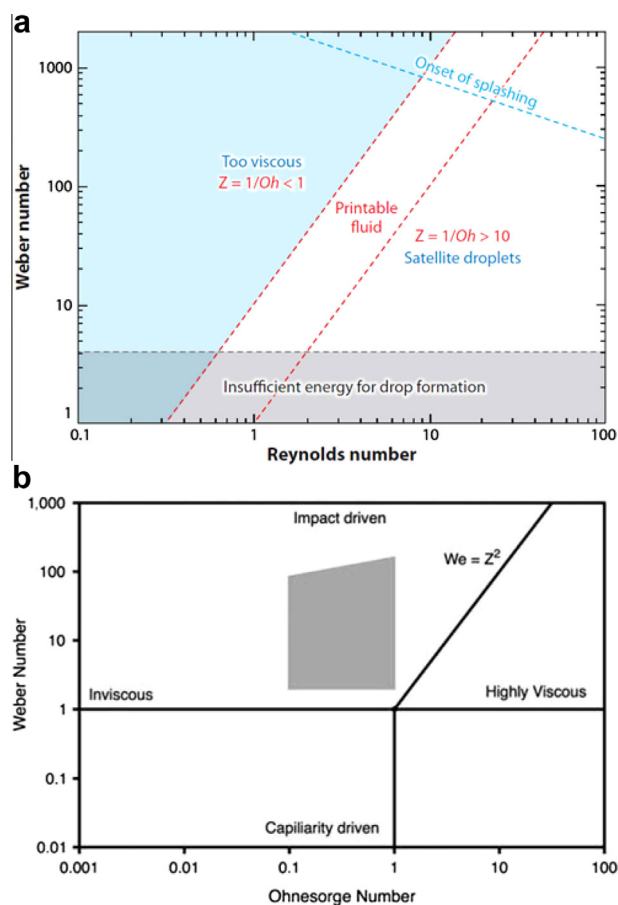


Fig. 2 – Influence of ink properties on (a) droplet formation (Reprinted from [27]. Copyright 2010 Annual Reviews) and (b) droplet spreading (Reprinted with permission from [28], modified from [30] and [27]. Copyright 2012 Emerald Group Publishing Limited). The shaded area in (b) is the region of high quality inkjet printing. (A color version of this figure can be viewed online.)

can eject from the nozzle, whereas low Z inks (low viscosity, high surface tension) will result in the formation of satellite droplets. Satellite droplets lead to blurred line edges and misplaced drops, ultimately leading to lower resolution. Therefore, when developing an ink formulation it is important to control these physical properties with the addition of surfactants, thickeners, stabilizers, and other additives.

The second stage of inkjet printing is droplet spreading, which is dependent on the interactions between the ink and the substrate. When the droplet contacts the surface of the substrate, inertial and capillary forces will influence the spreading behavior, while gravitational forces can be neglected [19]. Again, these forces are related by Re, We, and Oh, as shown in Fig. 2b. These parameters determine the surface energy and contact angle of the liquid droplets on the substrate and can be controlled by varying the viscosity, surface tension, and density of the ink, as well as the morphology, composition, and temperature of the substrate. Generally, the simplest method to ensure good spreading behavior, and therefore high resolution of the printing process, is a surface treatment on the substrate prior to printing [20].

During and after spreading, the solvent evaporates and leaves behind a solid film. Solidification is dependent on the solvent used and the temperature of the substrate. During solvent evaporation there is usually a significant decrease in volume, especially when the solid loading concentration is low, as is generally the case when printing carbon nanomaterials. This can be problematic if the ink is not well dispersed, as agglomeration of the solid content may occur, resulting in the formation of disconnected islands. The coffee-ring effect is another commonly encountered problem, in which the concentration of solids becomes higher at the droplet perimeter compared to in the center upon drying [21]. This can lead to fluctuations in the conductivity within a printed pattern and complications in device operation. A number of techniques have been shown to reduce this coffee-ring effect [22–26]. More detailed explanations of the major stages involved in inkjet printing can be found in references [27] and [28].

Inkjet formulations of carbon nanomaterials are usually comprised of functionalized carbon dispersed in a solvent, often with a surfactant. As an approximation, the solids in the ink should be less than one-fiftieth the size of the print head nozzles. Typically, inkjet printer nozzles have diameters on the order of tens of microns, so the graphene sheets and CNTs should have dimensions less than a few hundred nanometers to prevent clogging of the nozzles [29]. Agglomeration of the solids can also lead to clogging; therefore, the choice of solvent is very important to achieve a uniform dispersion. When the printer is not in use the solvent around the nozzles will evaporate, increasing the local viscosity and disrupting ideal droplet formation. The time for this gelation to occur is referred to as the latency time of the ink and is one of the major challenges of developing inks for inkjet printing [15]. Inkjet printer inks must have relatively low viscosity, compared to other techniques such as screen printing and 3D printing. The details of ink formulation are discussed in detail for nanostructured carbon materials in Section 3.

2.2. Screen printing

Screen printing is a technique using a mesh mask to deposit ink onto a substrate in a given pattern. The ink is placed on top of a thin plastic or metal screen that contains open areas that the ink is forced through with a squeegee (Fig. 3b). Screen printing is commonly used to apply patterns to textiles, wood, and glass. However, researchers have also used it to fabricate electronic devices, such as transistors [31,32], battery electrodes [5,33,34], solar cells [35–38], and fuel cells [39–41].

Screen printing differs from inkjet printing in that it is not an additive process, so there is more wasted material and generally less control of film thickness. However, it can be simpler to make films as the ink can be of a wider range of viscosities and surface tensions, whereas these parameters must be tightly controlled in the inkjet printing process. Usually screen-printed films are much thicker than inkjet-printed films. The film thickness after drying is directly proportional to the concentration of the coating solution, the paste volume of the screen, and the pick-out ratio, which

takes into account partial deposition of material. The pick-out ratio can be controlled by varying the squeegee force, printing speed, snap-off distance, snap-off angle, and ink viscosity [12]. In addition, because of the high pressures used to apply the ink to the substrate, the patterns are generally stable and unlikely to wash or rub off.

Similar to inkjet printing, screen printing uses inks composed of solids dispersed in a solvent. However, for screen printing, the inks have a higher viscosity and are less volatile. The solvent usually consists of water or an organic compound that is more stable at room temperature, making the drying process slower than for inkjet printing. Due to the required high viscosity and low volatility, the use of screen printing has been somewhat limited in the field of energy storage and conversion. However, low solid concentration and the coffee-ring effect are not problems when screen printing due to the high pressures used and the fact that the ink is not deposited as droplets. Additionally, screen printing can be adapted for roll-to-roll processing [35], meaning it could be a suitable fabrication technique for large-scale production of batteries, supercapacitors, fuel cells, and solar cells.

The quality of screen printed films depends on a number of factors, including mesh size, ink rheology, and the substrate used. Of these, ink rheology has the greatest effect and is the most important parameter to control. The ink viscosity and viscoelasticity are affected by the particle size [42], solid loading concentration [43], and inclusion of additives such as binders and dispersants [44]. It is critical to tune the binder concentration to ensure high quality prints. Not enough binder results in film cracking [45], whereas too much binder leads to printing problems due to the high viscosity and tackiness of the ink [41].

2.3. Transfer printing

Transfer printing involves patterning a material onto one substrate initially and then moving it to a second substrate. It has recently become a popular technique for printing a wide variety of materials, including graphene [46], carbon nanotubes [47], quantum dots [48], DNA [49], and metal nanostructures [50]. While inkjet and screen printing are limited to resolutions of approximately 12 μm and 40 μm [27,51], respectively, transfer printing can be used to pattern features below 100 nm [52,53].

The transfer printing process is shown schematically in Fig. 3c. First the material to be transferred is synthesized or patterned on its initial substrate. It is then brought into contact with the transfer substrate, generally a flexible elastomeric polymer, and peeled off from the first substrate. Then the transfer substrate with the transfer material is applied to the final substrate. In these last two steps, the temperature and pressure must be tightly controlled in order to get defect-free transfers. Lastly, the transfer substrate is removed and the transfer material remains.

Device fabrication can be performed separately from the assembly stage, which is beneficial for a number of materials and applications, especially graphene and flexible electronics. High quality graphene is usually synthesized by chemical vapor deposition (CVD) at high temperature, which is limited to only a few substrates such as silicon or copper. However,

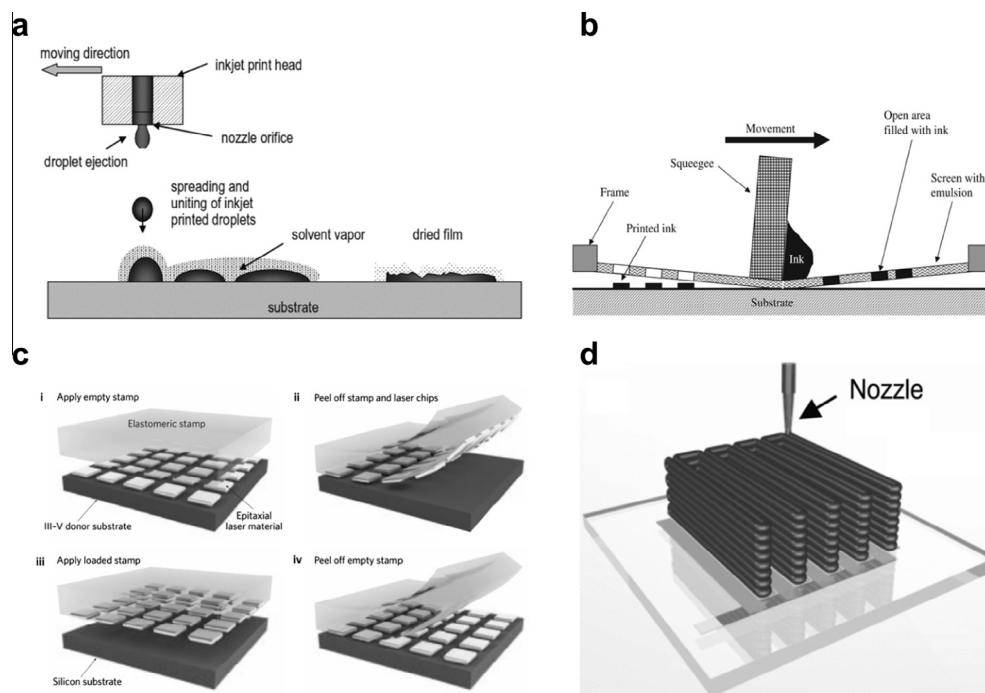


Fig. 3 – Schematic illustrations of (a) inkjet printing (Reprinted with permission from [13]. Copyright 2007 John Wiley and Sons), (b) screen printing (Reprinted with permission from [12]. Copyright 2009 Elsevier), (c) transfer printing (Reprinted with permission from [60]. Copyright 2012 Nature Publishing Group), and (d) 3D printing (Reprinted with permission from [55]. Copyright 2013 John Wiley and Sons).

many applications cannot use graphene in this form and it must therefore be transferred to a second substrate without introducing defects and compromising its quality. This is especially critical for flexible device fabrication, which are assembled on low melting point polymers, usually polyethylene terephthalate (PET). Transfer printing can accomplish this process without exposing the material to any chemicals or solvents that may damage it.

Transfer printing quality is determined by the types of transfer materials, substrate materials, and the working temperatures and pressures used. The adhesion between the transfer material and substrates must increase at each sequential printing step: the adhesion of the material with the final substrate must be greater than with the transfer substrate, which must be greater than with the initial substrate. This can be accomplished by optimizing the temperature and pressure applied during transfer, as well as by surface-treating with a fluorinated silane molecule [54].

2.4. 3D printing

Three-dimensional printing is a rapidly growing printing technique and is finding applications in an increasing number of fields. Recently it has been used to assemble a 3D battery [55], supercapacitor electrodes [56], tissue engineering scaffolds [57], strain sensors [58], and reduced graphene oxide nanowires [59].

3D printing of functional materials involves extruding material through a nozzle onto a substrate. The pattern is passed over multiple times to build up a three-dimensional structure (Fig. 3d). Similar to inkjet and screen printing, 3D

printing uses an ink comprised of solids dispersed in a solvent that dries upon contact with the substrate.

Minimal spreading and rapid drying are necessary for high quality 3D prints. This can be achieved by the addition of thickeners and volatile, low boiling point solvents. It is also necessary to ensure that the underlying layer does not completely dry before the next layer is printed on top of it by adding humectants [55]; otherwise poor adhesion between layers will result. By optimizing the ink's rheological properties, features below 10 μm have been achieved [61].

The implications of 3D printing are only beginning to be understood. Already this technique is changing the way people fabricate goods, decentralizing manufacturing and opening doors for innovative new products which could not otherwise be made. Carbon nanomaterials will play an important role, both as functional materials and as additives to 3D ink composites. 3D printing will be especially effective for energy storage and conversion device fabrication. For example, it is predicted that 3D-printed architectures can double the volumetric energy density of conventional batteries [55]. Table 1 provides a comparison of the four printing techniques discussed here. Furthermore, an outlook on the future of printing techniques for energy applications is given at the end of this review.

3. Printing nanostructured carbon

In this section, printing fullerenes, graphene, carbon nanotubes, and other nanostructured carbons is discussed. Details about ink formulations for inkjet and screen printing are given, with an emphasis on the surfactants, functional

Table 1 – Comparison of the four printing techniques discussed in this review.

	Inkjet printing	Screen printing	Transfer printing	3D printing
Minimum line width	~12 μm [27]	~40 μm [51]	<100 nm [52,53]	~10 μm [61]
Film thickness	10 nm [62]–500 μm [12]	400 nm [51]–500 μm [12]	0.34 nm [63]–20 μm [64]	>10 μm [61]
Drying time	Seconds	Minutes to hours	N/A	Seconds
Printing speed [12]	Slow to moderate	Moderate	Moderate to fast	Slow
Dimensions [12]	2D or quasi-3D	2D	2D	3D
Roll-to-roll compatible [12]	Yes	Yes	Yes	No
Solvent	Low viscosity, high volatility	High viscosity, low volatility	None	Very high viscosity, high volatility

groups, and solvents used to produce stable, jettable solutions. Transfer printing parameters are also discussed for graphene and CNTs. Table 2 summarizes the various ink formulations used for printing carbon nanomaterials.

3.1. Fullerenes

Buckminsterfullerene, comprised of 60 carbon atoms arranged into a hollow sphere, was first discovered in 1985 by Kroto, Heath, O'Brien, Curl, and Smalley at Rice University [65]. Since then, other fullerene molecules have been synthesized, including C_{20} , C_{70} , C_{76} , C_{80} , and C_{90} , which exhibit varying chemical, mechanical, and electrical properties. Fullerenes have gained considerable attention for energy, drug delivery, and cosmetic applications due to their high surface area, stability, radical scavenging properties, and ability to be easily functionalized.

The properties of fullerenes can be controlled by attaching different functional groups to their surface [66–68]. Functionalized fullerenes are highly effective n-type organic semiconductors and they are therefore commonly used in solar cells as electron acceptors and conductors [69]. [6,6]-Phenyl-C61-butyric acid methyl ester (PCBM) is by far the most common functional group for fullerenes used in energy applications. Extensive studies have examined mixtures of poly(3-hexylthiophene) (P3HT) with PCBM for polymer:fullerene blend organic solar cells.

PCBM was first synthesized in 1995 by Hummelen et al. [70], through a diazo addition process of which a typical example is shown in Fig. 4. Additionally, a second functional group can be covalently linked onto the other side of the fullerene molecule to produce bis-PCBM. These are well-known synthesis processes and fullerenes functionalized in this manner can be purchased for use without modification.

Solutions of P3HT:PCBM can be screen or inkjet printed. The most common solvents for this are chlorobenzene (CB), ortho-dichlorobenzene (o-DCB), and trichlorobenzene (TCB) due to the relatively high solubility of fullerenes [71]. In addition, these solvents are volatile and have low viscosities, ideal for inkjet printing. Teichler et al. [72] performed an extensive study to determine the best ink formulation for inkjet printing of PCBM. They tested both mono- and bis-PCBM, different polymers, varying concentrations of solids, and different ratios of solvents. Their study demonstrated that a concentration of 0.5 wt.% of mono-PCBM and a semiconducting polymer in 90:10 CB:o-DCB achieved the best films between 150 and 200 nm thick.

In another study, Neophytou et al. [73] optimized the inkjet printing process for P3HT:PCBM by varying a number of process parameters, including solution viscosity, substrate temperature, drop spacing, and nozzle-to-substrate distance. As expected, higher viscosities and substrate temperatures resulted in thicker layers and faster evaporation rates, respectively. Drop spacing affected film uniformity and thickness, as this parameter determines the total volume of material deposited within a given area. Too large a value resulted in inhomogeneous films, while smaller values led to thicker films. Lastly, the nozzle-to-substrate distance affected film quality, with larger distances producing satellite droplets and partial drying of the ink before it reached the surface. Therefore,

Table 2 – Summary of nanostructured carbon inks for printing.

Functionalization	Solvent	Carbon nanomaterial concentration (mg/mL)	Reference
<i>Fullerenes</i>			
PCBM	Tetralene or o-DCB + mesitylene	–	[13,15,138]
	CB	11, 22	[139]
	o-DCB	12, 24	[73]
	CB + TCB	3.8	[140]
mono-PCBM	CB + o-DCB	5.6–9.0	[72]
bis-PCBM	CB + o-DCB	5.6–9.0	[72]
<i>Graphene</i>			
None	Water	3.0	[141]
Surfactants			
Polyaniline	Water	–	[91]
Poly(styrene sulfonate)	Water	0.5	[91]
Polyelectrolyte	Water	–	[91]
N-vinyl-2-pyrrolidone:vinyl acetate copolymer	n-Butanol + isopropanol	1.4	[86]
Ethyl cellulose	Terpineol + ethanol	1.2	[18]
	Cyclohexanone + terpineol	3.4	[87]
	Terpineol	–	[142]
Carboxymethyl cellulose	Water + isopropanol	–	[143]
	Water	10	[144]
Functional groups			
p-Nitrobenzyl	Propylene glycol diacetate	3.0	[86]
1-(3-Aminopropyl)-3-methylimidazolium bromide	DMF, DMSO, water	–	[91]
PEDOT:PSS	Water	–	[145]
Graphene oxide	Water	9.0	[146]
	Water + ethylene glycol	–	[29]
	Water	0.9	[147]
	Water + polyethylene glycol	3.0	[141]
	Water + polyethylene glycol	8.0	[148]
	Water	4.4	[149]
	Water	2.0	[150]
CNTS			
None	DMF	4×10^{-5}	[112]
	NMP	0.003	[113]
Surfactants			
Sodium dodecyl sulfate	Water	0.2	[9]
	Water	0.3	[151]
	Water	2.0	[152]
	Water + methanol	0.05	[120]
Poly(2-methoxyaniline-5-sulfonic acid)	Water	–	[153]
Xanthan gum	Water	1.25	[154]
Gellan	Water	1.25	[154]
Functional groups			
Carboxyl groups	Water	0.26	[114]
	Water, water + PEDOT:PSS	0.5	[155]
Doping			
Nitrogen	Nafion solution	–	[156]
<i>Other carbons</i>			
Carbon black	NMP	20.6–41.2	[157]
Surfactants			
Carbon black + Nafion	Methanol	16.8	[125]
	Isopropanol + glycerol	20, 40, 50	[129–131]
	Isopropanol + ethylene glycol	20	[132]
	Water + ethylene glycol + isopropanol	–	[126]
	1-Propanol	–	[133]
	Various alcohols	20	[134]
Activated carbon + Triton X100	Ethylene glycol	33.3	[10]
Activated carbon + PMMA + PEG	Water	200	[123,124]

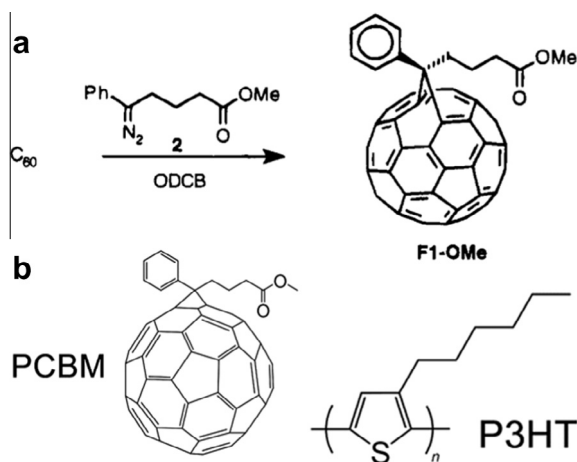


Fig. 4 – (a) The reaction for synthesizing PCBM from C₆₀. Reprinted with permission from [70]. Copyright 1995, American Chemical Society. (b) The structures of PCBM and P3HT. Reprinted with permission from [74]. Copyright 2014 The Royal Society of Chemistry.

smaller droplet travel distances are ideal for inkjet printing, as long as there is sufficient space for a full droplet to form.

Screen printing fullerene inks is more difficult, due to the low viscosity and high volatility of chlorobenzene solvents. Fullerenes do not exhibit high enough solubility in most solvents to attain sufficiently high viscosity for screen printing [75]. For this reason, there are only a few studies in which PCBM was screen printed [35,38,76,77].

Currently, the main method of functionalizing fullerenes for printing purposes is by synthesizing PCBM. This is because of its application in bulk heterojunction solar cells as an electron acceptor, which will be discussed later in this review. Because of the difficulty of dispersing fullerenes, only a few solvents are used for ink formulations. These typically consist of low viscosity, high volatility chlorobenzenes, which are excellent for inkjet printing but not for screen printing.

3.2. Graphene

Graphene is a promising new material, first isolated by Geim and Novoselov in 2004 [78], for which they were awarded the Nobel Prize in Physics in 2010. It is comprised of a single sheet of sp²-bonded carbon atoms that exhibits extraordinary properties. Graphene can withstand current densities up to 4×10^7 A/cm² [79], six orders of magnitude greater than copper [80] and has a theoretical surface area of 2630 m²/g [81], which rivals that of activated carbon. It also has outstanding mechanical and optical properties. For these reasons, it is gaining popularity in energy storage and conversion applications, such as battery electrodes, supercapacitors, fuel cell catalyst supports, and solar cells.

For inkjet and screen printing, graphene nano-platelets prepared by the reduction or exfoliation of graphene oxide (GO) are typically used whereas single layer, CVD-prepared graphene can only be printed by transfer printing. Inkjet printing is by far the most common printing technique used

for graphene. Proper selection of solvent is very important to achieve high quality prints. However, the best solvents for dispersing graphene, dimethylformamide (DMF) and N-methylpyrrolidone (NMP), are toxic. NMP also has a higher viscosity than water, meaning that graphene nanosheets dispersed in NMP experience higher frictional forces and a greater sedimentation coefficient [82,83]. This leads to lower yields when preparing the inks, due to decreased sedimentation during centrifugation [84].

For these reasons, water is the most common solvent used for inkjet printing of graphene, even though its viscosity (1 cP at 20 °C) is too low for ideal jetting (~10 cP). Additives, such as polymer surfactants, increase the ink's viscosity to usable levels. However, in water, pristine graphene tends to agglomerate due to the strong van der Waals forces between sheets [85]. Therefore, to print, either (1) a surfactant must be added to the ink, (2) the graphene must be functionalized, or (3) it must first be printed as GO and subsequently reduced to graphene after printing. The first two approaches involve stabilizing the surface to prevent agglomeration, while the third involves printing the more readily-dispersible GO.

Surfactants prevent the agglomeration of graphene sheets by electrostatic repulsion or steric hindrance. Polymer surfactants, in particular, also help to increase the viscosity of the solution. However, surfactants decrease the electrical conductivity of the printed films because of increased contact resistance between graphene sheets [86]. One approach is to use a post-annealing process to remove the residual surfactant molecules after printing.

Fig. 5 shows the steps used by Secor et al. [87] to prepare ethyl cellulose (EC)-stabilized graphene ink. The ethyl cellulose molecules were readily removed with a post-annealing step at 250 °C and the treated graphene film achieved a conductivity of 2.5×10^4 S/cm, which is twenty times greater than the printed graphene films with residual surfactant remaining (1.25×10^3 S/cm [86]). However, this annealing step limits the potential substrates to those with high melting temperatures, preventing the use of most flexible substrates.

Functionalizing graphene with covalently bonded molecules is another common technique used to attain good dispersions and optimal jetting. It avoids the increased sheet-to-sheet contact resistance prevalent when using surfactant molecules; functional groups instead increase the charge carrier concentration and thus the conductivity of the graphene [88]. Electron donor groups, such as pyrene-1-sulfonic acid sodium salt [89] act as n-dopants, while electron acceptor groups, such as 3,4,9,10-perylenetetracarboxylic diimide bis-benzenesulfonic acid [89] and perylenebisimide [88] act as p-dopants. These are generally large planar aromatic structures that are strongly bound to the graphene sheets by π - π interactions without affecting electronic conjugation [90]. Table 2 summarizes the various surfactants and functional groups used by researchers to stabilize graphene dispersions for inkjet printing.

Fig. 6 shows the surfactant and functional molecules used by Wei et al. [91] to prepare graphene inks for printing. Graphene was functionalized with 1-(3-aminopropyl)-3-methylimidazolium bromide ionic liquid (IL), polyaniline, poly[2,5-bis(3-sulfonatopropoxy)-1,4-ethynylphenylene-alt-1,4-ethynylphenylene] (polyelectrolyte), and poly(styrene

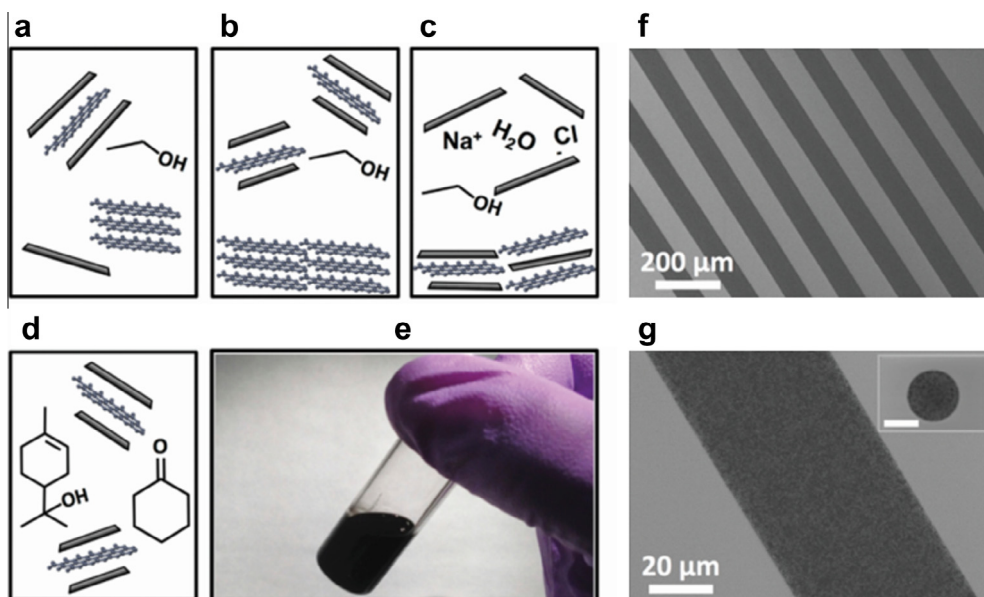


Fig. 5 – Graphene ink preparation used to inkjet print high conductivity, flexible graphene patterns. (a) First, graphite was exfoliated by probe sonication in ethanol/EC. EC is represented by the gray bars surrounding the graphene sheets. (b) Then the larger flakes were removed by centrifuging, to prevent clogging of the nozzles. (c) Next the graphene/EC was flocculated out of solution by the addition of salt and (d) the obtained powder was dispersed in cyclohexanone/terpineol. The prepared ink (e) was printed on a surface-treated substrate, demonstrating excellent jetting properties and patternability. (f, g) The combination of surfactant, surface treatment, and post-annealing process resulted in very uniform films with high conductivity. Reprinted with permission from [87]. Copyright 2013 American Chemical Society. (A color version of this figure can be viewed online.)

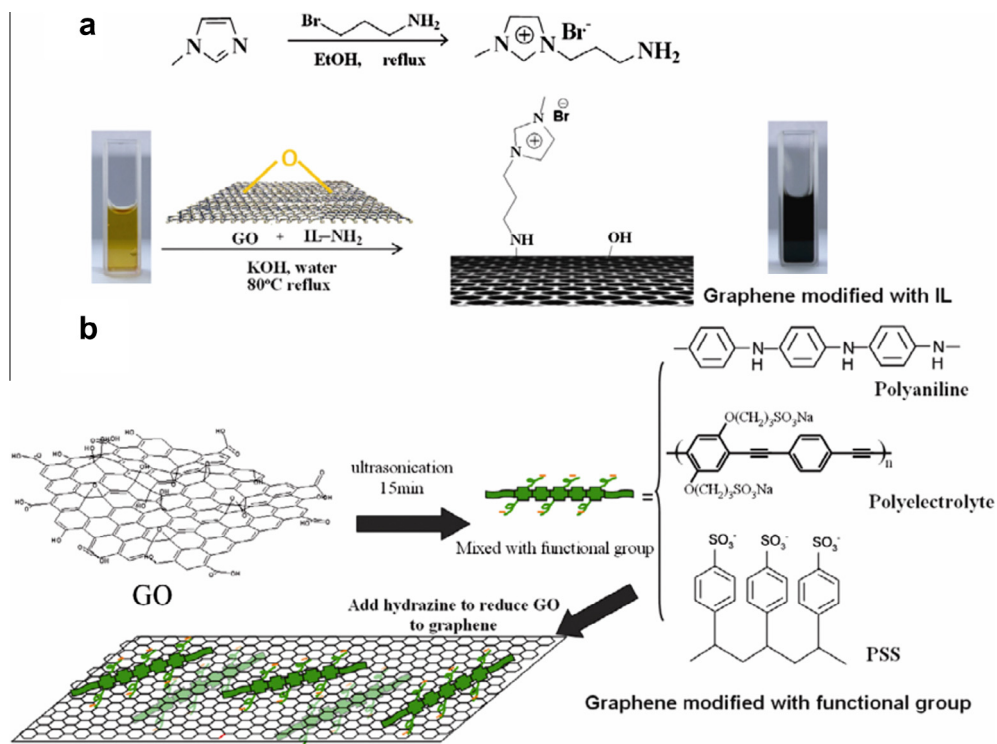


Fig. 6 – Graphene inks stabilized by different functional groups and surfactants. Graphene modified with (a) an ionic liquid and (b) different functional groups: polyaniline, polyelectrolyte, and PSS anions. Reprinted with permission from [91]. Copyright 2011 IOP Publishing. (A color version of this figure can be viewed online.)

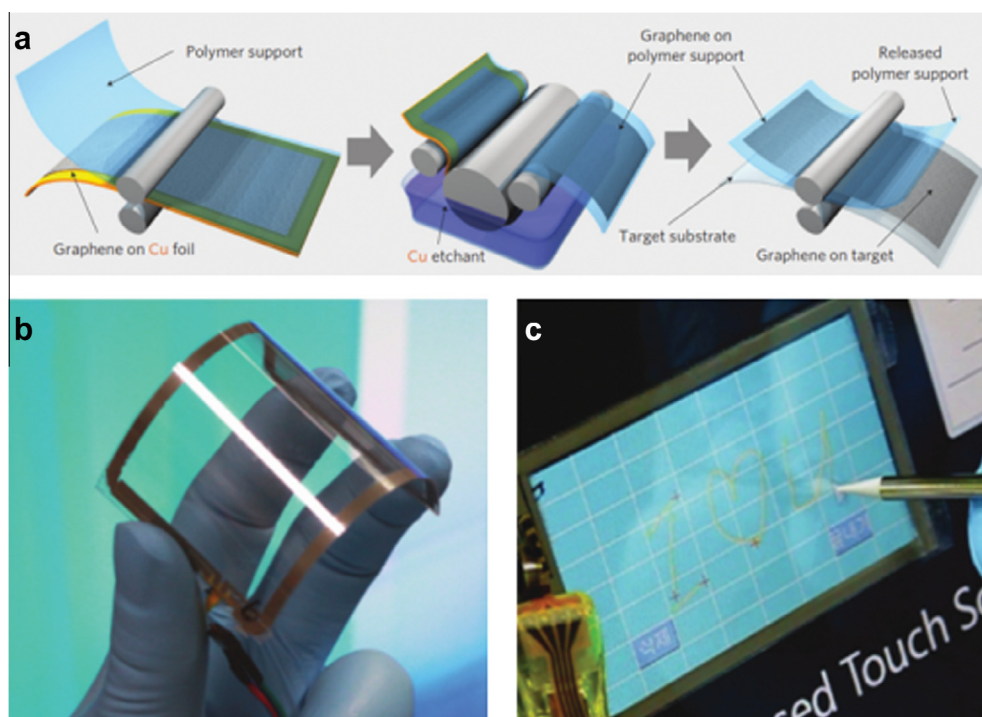


Fig. 7 – (a) Illustration of a roll-to-roll transfer printing process for large-scale graphene films. (b) and (c) Assembled graphene screen panel exhibiting high degree of flexibility and touch sensitivity. Reprinted with permission from [63]. Copyright 2010 Nature Publishing Group. (A color version of this figure can be viewed online.)

sulfonate) (PSS) to create uniform dispersions in water. Only the ionic liquid (Fig. 6a) was covalently bonded to the carbon lattice. The other polymer molecules acted as surfactants to stabilize the graphene sheets in water (Fig. 6b). These modifications increased the surface energy of graphene, making it more hydrophilic. The surfactant-modified inks had the lowest contact angles and therefore the best wettability on the silicon substrate.

Printing graphene oxide is a simpler alternative to using surfactants or functional groups to attain good dispersions of graphene. The oxygen-rich GO is readily-dispersed in water at higher concentrations than graphene-based solutions, meaning that less printing passes are necessary to attain uniform films or sufficient thickness. However, GO is electrically insulating and reducing it into reduced graphene oxide (rGO) does not achieve the high conductivities of pristine graphene [92]. Reduction is typically done by exposure to hydrazine followed by annealing at high temperatures (>300 °C) [92–94] which is often above the melting temperature of the substrate, especially for flexible electronics applications. Nonetheless, printing GO is common due to its simplicity and can be used for applications where ultrahigh conductivity is not necessary.

As stated in Section 2.1, the graphene sheet dimensions must be less than a few hundred nanometers to prevent the inkjet nozzles from becoming clogged. Decreasing the size of the individual graphene nano-platelets increases the contact resistance between them [95], ultimately resulting in the printed films having a lower conductivity. Therefore when high conductivity is a priority, transfer printing is preferred.

Fig. 7 shows a roll-to-roll transfer printing process for the transfer of large graphene films to flexible substrates. First,

graphene is grown on copper foil using a standard CVD process. Then a polymer substrate is adhered to the graphene sheet and the copper is etched in an ammonium persulfate solution. Finally, the graphene is transfer printed onto the target flexible substrate for use in bendable displays (Fig. 7b and c). This method has been used to print large 30-inch films of single-layered graphene on flexible polymer substrates and in the future may be used as a scalable fabrication technique for the transparent electrode material in solar cells. Another transfer printing method for graphene was recently reported by Hallam et al. [96], which enabled the transfer of graphene films with periodic folds. This technique, called GraFold printing, produces folded graphene without damaging or functionalizing the graphene and can be used to alter its carrier transport properties.

As discussed above, there are trade-offs between dispersibility and the properties of the graphene films attained after printing. Generally, to make a well-dispersed ink, surfactants or functionalization must be used, or it must first be printed as graphene oxide with a subsequent reduction step on the substrate. However, these techniques can lead to lower conductivity and limit the substrates that can be used.

Doping graphene, by replacing some carbon atoms with nitrogen, boron, sulfur, or phosphorous atoms, may be the solution to attaining the highest quality printed graphene films. Doped graphene is more readily-dispersed in water and exhibits higher conductivity than pristine graphene [97]. Therefore, it should produce excellent jetting properties without introducing surfactants or functional groups bonded to the surface of graphene. Nitrogen-doped graphene has been used for a number of applications with improved

performance over pristine graphene, including fuel cell catalyst supports [98,99], lithium-ion battery electrodes [100–102], and supercapacitors [103–105].

3.3. Carbon nanotubes

CNTs are cylindrical molecules comprised of a hexagonal lattice of carbon atoms. Like graphene, they exhibit extraordinary thermal conductivity [106] and mechanical strength [107]. Depending on their structure, they can exhibit conducting or semiconducting behavior [108]. CNTs can be grown to lengths of over 18 cm, having length-to-diameter ratios of over $10^8:1$ [109]. Because of these amazing properties, CNTs have a wide range of applications in state-of-the-art electronic devices, such as transistors, batteries, supercapacitors, and fuel cells.

As with graphene, inkjet printing is the most popular printing technique for CNTs. The best solvents for dispersing CNTs are DMF and NMP [110,111] but, as stated above, there are a number of issues with using them for inkjet printing. Again, water is the most popular choice of solvent, and surfactants are added into the ink formulation and functional groups are covalently bonded onto the CNTs to improve their dispersibility. Heteroatom doping into the carbon lattice is also an effective strategy for ink preparation. The different functionalization techniques used to prepare CNT inks are summarized in Table 2.

It should be noted that it is possible to attain acceptable films without any functionalization; however, these typically require very low concentrations of CNTs. For example, Okimoto et al. [112] fabricated CNT thin film transistors entirely by inkjet printing without the use of surfactants or functional groups, by dispersing CNTs in DMF at 0.04 $\mu\text{g/mL}$. Additionally, Beecher et al. [113] were able to print CNTs without the use of a surfactant by using NMP with a CNT concentration of 0.003 mg/mL.

Fig. 8 shows a typical procedure for functionalizing CNTs with carboxyl groups. First, multi-walled carbon nanotubes (MWCNTs) were refluxed with nitric acid, creating carboxyl, hydroxyl, and carbonyl groups on the outer surfaces. Further oxidation was performed with potassium permanganate in perchloric acid to produce additional carboxyl groups. These functionalized CNTs can be easily dispersed in water. However, the inkjet-printed functionalized CNT films exhibited relatively high sheet resistances of 40 $\text{k}\Omega/\square$ even after 90 printing passes [114], due to the increased contact resistance between CNTs caused by the non-conductive, oxygen-containing functional groups.

Doped CNTs may be a better alternative. They exhibit a number of improved properties over their pristine counterparts, including higher surface energy [116], higher chemical activity [117], and better electronic and optical properties [118]. However, there are very few studies in which doped CNTs are printed, which may be due to the relative novelty of both printing techniques for CNTs and CNT doping.

To prevent clogging of the nozzles, relatively short CNTs must be used. Typically, those with lengths under 1 μm are favored. To ensure longer nanotubes are absent, these inks are usually pre-filtered using filter paper or syringe filters. Nevertheless, this limits the conductivity of the printed films, since it increases the number of contact resistance points between CNTs. To increase the conductivity, longer CNTs must be printed using techniques other than inkjet printing, such as transfer printing.

Kang et al. [119] developed a transfer-printing process for depositing aligned single-walled carbon nanotubes (SWCNTs). Complex CNT patterns were first grown by CVD on quartz by patterning the catalyst particles. They were then transferred to a SiO_2/Si substrate by using a transfer substrate made of gold and either polyimide or polyvinyl alcohol. This process did not introduce any defects or change the coverage or layout of the CNT patterns. The authors were also able to align the CNTs in different directions via a two-step transfer printing process. Rotating the stamp by 90° produced crossbar arrays and rotating by 60° led to triangular lattices. This allowed them to tune the conductivity of the transferred patterns, with the crossbar arrays exhibiting conductivities about 18.5 times higher than randomly-oriented CNT films.

However, tuning the conductivity involved multiple transfer printing steps. By using a controlled flocculation process, Meitl et al. [120] were able to control the thickness and conductivity of SWCNT films in a single deposition step. Using this technique enabled them to finely tune the density of SWCNTs on the substrate, from a few nanotubes per square micron to thick films. By adding a transfer-printing process, they also demonstrated the ability to pattern CNTs onto flexible substrates. Fig. 9 shows the printing process. An ink of methanol and an aqueous solution of SWCNTs were applied to a rotating patterned poly(dimethylsiloxane) (PDMS) stamp via a controlled flocculation method. By controlling the time of the deposition process, the thickness of the films could be varied. After deposition onto the PDMS substrate, the CNTs were patterned onto different substrates including a capillary tube to model the ability of patterning on flexible substrates.

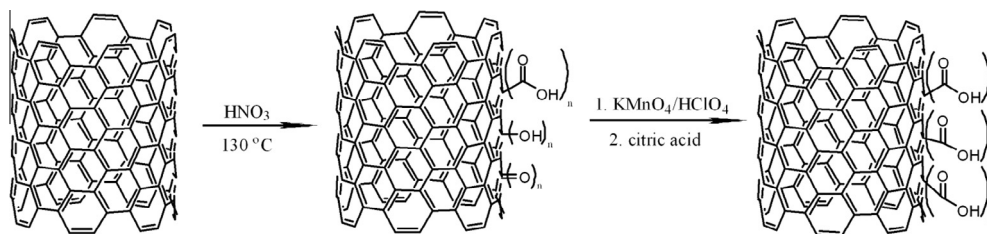


Fig. 8 – Functionalization of MWCNTs with carboxyl, hydroxyl, and carbonyl groups to make them dispersible in water for inkjet printing. Reprinted with permission from [115].

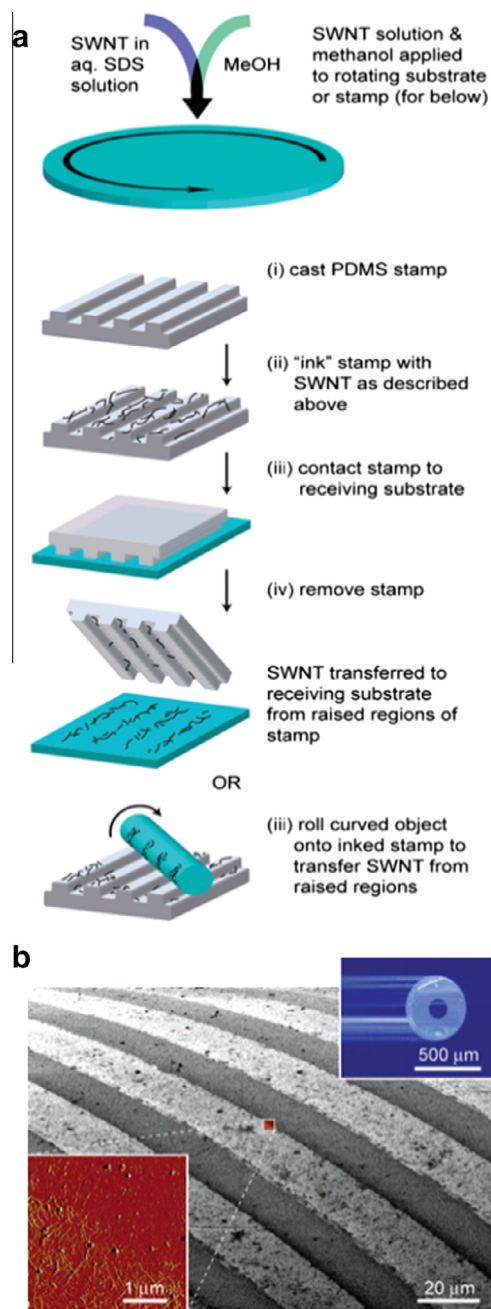


Fig. 9 – (a) Solution casting and transfer printing process for depositing SWCNTs. (b) SEM image of lines printed onto a capillary tube with a diameter of 500 μm, shown in the top-right inset. Bottom-left inset is an AFM amplitude image showing the printed SWCNT line edge. Reprinted with permission from [120]. Copyright 2004 American Chemical Society. (A color version of this figure can be viewed online.)

Overall, printing graphene and CNTs have similar requirements. In their pristine form, both are virtually indispersible in water and require functionalization for inkjet printing. Surfactants, functional groups, and doping can improve the dispersibility of carbon nanomaterials. However, the limitations to the maximum sizes of the carbon content in inkjet-printed inks increase the contact resistance and reduce

the conductivity of the entire printed film. When conductivity is a priority, transfer printing may be used. These printing techniques have the potential to drastically change the way electronic devices are fabricated in the near future, enabling the large-scale assembly of functional materials where patternability and thickness control are required.

3.4. Other carbon materials

Activated carbon and carbon black are both used in enormous quantities for industrial applications ranging from additives in rubber and plastic to pigments in ink. Both exhibit physical and electrical properties that make them useful in a variety of energy storage and conversion devices. Porous activated carbon is commonly used for supercapacitor electrodes due to its high surface areas, which can reach up to 3000 m²/g [121], while carbon black is a common catalyst support for fuel cells due to its high electrical conductivity, surface area, and reasonable corrosion resistance [122]. For printing, these materials are attractive due to their low cost and ability to modify and control colors and tones. Carbon black in particular is often used in electrostatic toners, lithographic ink, and black inkjet printer ink.

One of the drawbacks of using these nanostructured carbons is their poor dispersibility in water while nonaqueous solvents typically have viscosities that are too low to be inkjet or screen printed. In order to print, then, these nanostructured carbons must be functionalized or a surfactant must be added to the ink. Activated carbons have been inkjet printed [10] and screen printed [123,124] by dispersing them in water with surfactants. These carbon materials can be more readily-dispersed at high concentrations compared to graphene and CNTs, making it easier to deposit thick films.

Carbon blacks are the most popular material for fuel cell catalyst supports and have been printed into catalyst layers [125,126]. The use of carbon black for methanol fuel cells [127] and for precious metal-free catalysts [128] has also been reported. Numerous studies have demonstrated its efficacy as a printable nanostructured carbon material for both inkjet [125,126,129–133] and screen [134] printing of functional devices. In most of these cases, a mixture of water and an alcohol are used as a solvent.

One potential alternative to the use of surfactants may be doping carbon with nitrogen to improve its dispersibility in water. Nitrogen-doped carbon black and mesoporous carbon has already been demonstrated for fuel cell applications, where it exhibited similar oxygen reduction performance compared to in its undoped state [127,135–137]. While there are myriad other carbon nanomaterials, studies of their suitability for printing has not yet been carried out.

4. Energy applications of printed nanostructured carbon

Many studies have focused on adapting the printing technologies discussed above for fabricating energy storage and conversion devices. Components of batteries, supercapacitors, fuel cells, and solar cells can be replaced with carbon nanomaterials to increase performance. By producing these parts

with printing and solution processing techniques, their properties can be finely controlled. This section details the work to date on fabricating carbon-based battery electrodes, supercapacitor electrodes, fuel cell catalyst supports, and organic photovoltaic cells using printing techniques.

4.1. Batteries

Today, lithium-ion batteries (LIBs) are the most widely used portable energy storage devices, with the global market estimated to grow from \$878 million in 2010 to \$8 billion in 2015 to \$26 billion in 2023 [158]. Commercial LIBs are composed of a graphite negative electrode (anode) and a lithium metal oxide positive electrode (cathode) separated by a polymer separator immersed in nonaqueous liquid electrolyte. During charging, lithium ions are extracted from the cathode, migrate across the electrolyte, and intercalate between graphite layers in the anode, forming LiC_6 . During discharge, the reverse electrochemical reaction occurs – lithium ions deintercalate from the graphite and reinsert into the cathode. These processes produce and consume electrons via oxidation and reduction reactions, respectively. The electrons are then free to move around the external circuit supplying energy to an external load (discharging) or storing their energy as chemical potential energy (charging). To the best of our knowledge, other advanced electrochemical energy conversion systems (e.g. Li–S batteries, sodium-ion batteries, and metal–air batteries) or their components have not been fabricated by printing techniques to date. Therefore, this section will focus exclusively on LIBs.

LIBs are widely adopted in a variety of portable electronics, such as cell phones, cameras, and laptops, and are becoming increasingly used in electric vehicles. This is due to their unique merits, such as high energy density, low self-discharge rate, no memory effect, and decreasing price. There are four main requirements that LIBs must meet to achieve high performance: (1) high capacity and electrically conductive electrodes. (2) An electrolyte with high ionic conductivity; a minimum ionic conductivity of 10^{-3} S/cm is required for commercial batteries [159]. (3) Reasonable charge/discharge rates; for consumer electronic applications, LIBs must be able

to fully charge within a few hours and be able to deliver energy in short timeframes for periods of high power demand. (4) High cycling stability; cells must have long lifetimes for portable electronic devices.

Carbon-based materials have been used as anode materials since the birth of LIBs, while nanostructured carbon materials are believed to be the choice for future LIBs. For example, high quality, pristine graphene can form Li_2C_6 and even Li_4C_6 compounds [160,161], giving theoretical capacities of 744 mAh/g and 1448 mAh/g, respectively. By using printing techniques, nanostructured carbon LIB electrodes can be patterned to any desired shape with precise control over the thickness.

While others have inkjet and screen printed metal oxide LIB anodes with carbon black as a conducting agent [2,3,5,6,33,162], Kim et al. [163] were the first to print fully-carbon anodes. They developed an ink formulation comprised of mesocarbon microbeads (MCMBs), carbon black, and PVDF-HFP binder dispersed in dibasic ester. This ink was then spread onto a glass slide and irradiated with a laser to form 3D pixels of electrode material, by a laser printing technique. Thickness could be controlled by varying the number of laser pulses. This technique was used to create patternable thick carbon films. The high porosity of the MCMBs led to increased ionic conduction through the electrodes, resulting in higher areal capacities compared to other thin-film microbatteries.

Thickness control is important for tuning the amount of active material in the electrode. This is especially true for thin film, flexible batteries [164,165]. The capacity of a cell is directly related to the mass of the material present, so the thicker the electrode the greater its capacity. Flexible LIBs can be fabricated by printing thin films of nanostructured carbon onto a flexible substrate. Wei et al. [166] developed a flexible solid-state LIB made with graphene inks (Fig. 10), comprised of anatase titanate (TiO_2) nanoparticles mixed with graphene sheets modified with either n-type or p-type anionic groups dispersed in water. The n-type functional groups consisted of poly(styrenesulfonate) (PSS^-) and poly[2,5-bis(3-sulfonatopropoxy)-1,4-ethynylphenylene-alt-1,4-ethynylphenylene] sodium salt (PPE-SO_3^-), while polyaniline was used for p-type modification. These chemical groups

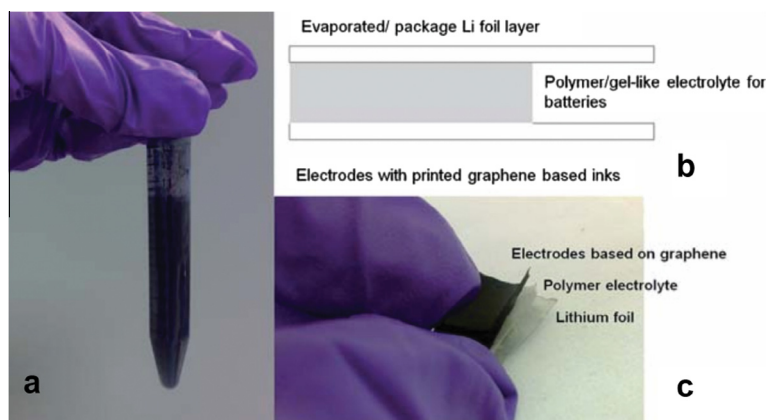


Fig. 10 – (a) Modified graphene ink for printing flexible solid-state lithium battery electrodes. (b) Schematic diagram showing the major components of the cell. (c) Demonstration of the flexibility of a printable graphene electrode. Reprinted with permission from [166]. Copyright 2011 The Royal Society of Chemistry. (A color version of this figure can be viewed online.)

helped stabilize the graphene dispersions in water, allowing them to be printed without agglomeration and subsequent clogging of the nozzles. The printable electrodes exhibited stable cycling performance at 240 mAh/g for 100 cycles, which is comparable to other flexible LIBs [164]. Flexible LIBs typically have lower capacities than their rigid counterparts due to the low ionic conductivity of the solid-state electrolytes used [167].

In addition to these TiO₂/graphene electrodes, mixtures of other metals and metal oxides with graphene are being explored for their potential application in LIBs. Two of the most promising anode materials are silicon and tin oxide, which have theoretical capacities of 4200 mAh/g and 990 mAh/g, respectively. However, upon lithiation and delithiation, these materials undergo large volume expansion and contraction, with volume changes up to 400% for silicon [168] and 200% for tin oxide [169]. This causes the particles to crack and the electrodes to degrade during cycling, decreasing the battery's cycle life. To overcome this problem, researchers have combined silicon [170] and tin oxide [171,172] with graphene sheets to reduce the strain on the nanoparticles during volume expansion. Intimate bonding between the nanoparticles and graphene sheets increases the cycle life and capacity of these anodes. To date, these composite anodes have not been fabricated by printing techniques; however, it should be a relatively straight-forward process to develop inks from these materials and use them for large-scale production of high performance, flexible LIBs.

In addition to LIB electrodes, nanostructured carbon can be used to replace conventional battery current collectors. In commercial LIBs, metal foil current collectors account for 15–25% of the mass of the battery [173] without contributing to lithium storage. This means that the gravimetric energy density can be dramatically increased by using lower density materials. CNTs are excellent current collectors for LIBs due

to their high conductivity, mechanical robustness, and low density (0.04 mg/cm²). Additionally, CNT-based current collectors exhibit stronger adhesion with the electrochemically active material, and therefore lower contact resistance, compared to their metal counterparts [174]. The overall battery weight is reduced due to their low density and since CNTs are electrochemically active, they can both contribute to lithium storage and act as the current collector in a single cell.

Dispersions of CNTs in water or other solvents allow for simple fabrication of large area current collectors. Kiebele et al. [175] designed a battery with a current collector made of printed SWCNTs. The current collector and electroactive materials are combined in a single layer, reducing the overall weight and volume of the cell, as well as the number of manufacturing steps required during assembly. Using this design, the gravimetric and volumetric energy densities of LIBs can be dramatically improved.

The greatest challenge for fully printed batteries is the development of a printable electrolyte. Ideally, a fully integrated process will be used in the future, in which the anode, electrolyte, and cathode are sequentially printed on top of one another. However, liquid electrolytes suffer from leakage when the battery is flexed along with safety concerns regarding their flammability. They also limit how the cell can be designed, due to the requirement of a separator. Gel and polymer electrolytes, on the other hand, are mechanically stable, leak-proof, less toxic, and are less flammable. However, their ionic conductivities are very low, severely limiting their use in modern LIBs. Therefore many research groups are currently focused on developing high conductivity, flexible polymer electrolytes. Table 3 shows a number of candidate LIB electrolytes that may be suitable for printing.

To date, few printable battery electrolytes have been reported [176,177]. Gel polymer electrolytes [178] are most promising, as they generally exhibit higher ionic conductivities

Table 3 – Potential LIB electrolytes for printing techniques.

Electrolyte	Ionic conductivity (S/cm)	Temperature (°C)	Reference
Liquid (LiPF ₆ in 1:1 EC/DMC)	1 × 10 ⁻²	25	[179]
Organic gel (LiClO ₄ in EC/PC + PAN)	2 × 10 ⁻³	25	[178]
Gel polymer (LiTFSI + PVdF-HFP)	2 × 10 ⁻³	20	[180]
Gel polymer (PYR ₁₄ TFSI + PAN/PMMA)	3.6 × 10 ⁻³	25	[181]
Gel polymer (LiPF ₆ in EC/PC + ETPTA + HMPP)	1.5 × 10 ⁻³	30	[182]
Polymer (LiTFSI + PEO)	1 × 10 ⁻³	85	[183]
Block co-polymer (PS-PEO/LiTFSI + SEO)	1 × 10 ⁻⁴	90	[184]
Semi-IPN (LiTFSI in SN + ETPTA + PVdF-HFP + HMPP)	3.5 × 10 ⁻³	30	[185]

Abbreviations: EC – ethylene carbonate, DMC – dimethyl carbonate, PC – propylene carbonate, PAN – poly(acrylonitrile), LiTFSI – lithium bis(trifluoromethylsulfonyl)imide, PVdF-HFP – poly(vinylidene fluoride-co-hexafluoropropylene), PYR₁₄TFSI – N-methyl-N-butylpyrrolidinium bis(trifluoromethylsulfonyl)imide, PMMA – poly(methyl methacrylate), ETPTA – ethoxylated trimethylolpropane triacrylate, HMPP – 2-hydroxy-2-methyl-1-phenyl-1-propanone, PEO – poly(ethylene oxide), PS – polystyrene, SEO – poly(styrene)-block-poly(ethylene oxide), SN – succinonitrile.

and are in a liquid state at some point during their synthesis. This means that they could be printed as a liquid and then solidified by evaporation or post-treatment. In these cases, it may not be possible to reduce the viscosity enough to achieve good jetting for inkjet printing, but they should be suitable for screen and 3D printing techniques.

Fabrication of battery components by printing is still a relatively new concept and more work must be done to prove its efficacy. Printing techniques are more suited for fabricating smaller batteries for consumer electronics; however they may also be feasible for manufacturing larger cells for electric vehicles by using a scaled-up printer or roll-to-roll technology. The true power of battery printing will be realized with 3D printing techniques, in which electrodes can be readily patterned into micro- and nano-structures [186]. Interdigitated electrodes can be used to minimize the ionic path length and achieve high charge/discharge rates, as well as increase the volumetric energy density by using the limited space within the cell [55]. And 3D printers are able to extrude much higher viscosity fluids than inkjet printers, making it possible to print polymer electrolytes and fabricate fully-printed batteries.

It should be noted that the application of printing technology to other advanced battery systems, including lithium–sulfur, sodium-ion, and metal–air, has not yet been demonstrated. However, the printing techniques discussed here may also be suitable for these batteries, which involve the use of different types of carbon-based materials. For example, carbon encapsulated sulfur (C–S) composite materials are the most commonly used electrodes for Li–S batteries in the state-of-the-art. These sphere-shaped carbon blacks used as the sulfur host have a similar morphology to the common carbon blacks used in inkjet printing. So it can be expected that such materials can be easily adopted for printed electrodes. Additionally, various printed materials can be used for the electrode in sodium-ion batteries, which have similar electrochemistries to Li-ion batteries. Additionally, porous carbon cathodes are indispensable in metal–air cells. Printing technology can not only ensure the large-scale and uniform fabrication of these air cathodes, but also realize a 3D-structured air electrode to efficiently accommodate the discharge products. In brief, the potential of printing technology for batteries is still far from being fully realized.

4.2. Supercapacitors

While LIBs can store large amounts of energy, one limitation is their relatively low power density. This results in long charge times and the inability to draw large amounts of energy in a short period of time. Supercapacitors (SCs), on the other hand, exhibit very high power densities with lower energy densities. They can therefore be used in combination with batteries, or as stand-alone energy storage devices. Additionally, SCs can operate in freezing conditions [187], making them effective for low temperature applications.

There are three main classifications of SCs: electric double-layer capacitors (EDLCs), pseudocapacitors, and hybrid capacitors, which are a combination of the first two types. EDLC and hybrid capacitor electrodes are typically comprised of carbon, while pseudocapacitor electrodes are usually made

of metal oxides or conductive polymers [188]. For this reason, we will focus on the nanostructured carbon materials used in EDLC and hybrid capacitors in this section.

Electric double-layer capacitors typically consist of two parallel plates of conducting material separated by a liquid electrolyte solution. Upon an applied voltage, the plates become oppositely charged and an electric double layer forms on their inner surface by the movement of ions in the electrolyte. This stored energy can then be released as electrical energy to an external load at very high rates.

SCs have commonly been used for electronic memory protection and small-scale power storage. Recently, there has been increased demand for high performance power devices for applications in electric vehicles, uninterrupted power supply systems, smart grid power quality control, and transmission line stability [189]. For these applications, SC electrodes must have high electrical conductivities and large surface areas, while the entire device must have high capacitance, long cycle life, high specific power density, and low equivalent series resistance.

Parallel plate SC electrodes are conventionally comprised of activated carbon, which is a porous form of carbon with extremely high surface area (500–3000 m²/g) [121]. Pech et al. [10] demonstrated an inkjet printing process in which activated carbon was deposited onto patterned gold current collectors. However, activated carbon has relatively low electrical conductivity (0.1–1 S/cm) [190] and a wide range of pore sizes, the smallest of which do not contribute to charge storage [191]. Carbon nanomaterials, with similar surface areas and better conductivities are therefore ideal candidates to replace activated carbon and recently many studies have shown the efficacy of using graphene [192–196] and CNTs [197–200] as SC electrodes. Additionally, CNT networks are mesoporous, allowing for easy electrolyte diffusion which decreases the equivalent series resistance and increases the capacitor's maximum power [198].

Printing is an effective technique for fabricating thin, flexible SC electrodes made of nanostructured carbon [188]. Inkjet printing and spray casting make it possible to deposit electrode materials on large-area flexible substrates. Through patterning and printing multiple layers, the electrical properties of the SC can be controlled, allowing one to tune the capacitance for the desired application.

An inkjet printed CNT-based SC is shown in Fig. 11. In this study, a dispersion of SWCNTs in water with sodium dodecyl sulfate surfactant was inkjet-printed onto a cloth fabric. The SEM images show a dense network of tangled CNTs coating the individual fibers. A polymer electrolyte was pressed between two coated fabrics to form a flexible SC (Fig. 11d) that displayed excellent capacitance for over 1000 cycles [9]. The major drawback of this fabrication technique is the very high number of prints required to achieve a suitable thickness and sheet resistance. For the inkjet-printed SC on cloth fabric shown, 190 layers were necessary to obtain acceptable properties. Thus, improvements to this process must be made before commercialization and scalable production is possible.

Using a similar inkjet printing method, Hu et al. [152] fabricated SWCNT SC electrodes on a single sheet of Xerox paper. The paper was first treated with PVdF to prevent CNTs from penetrating through to the other electrode on

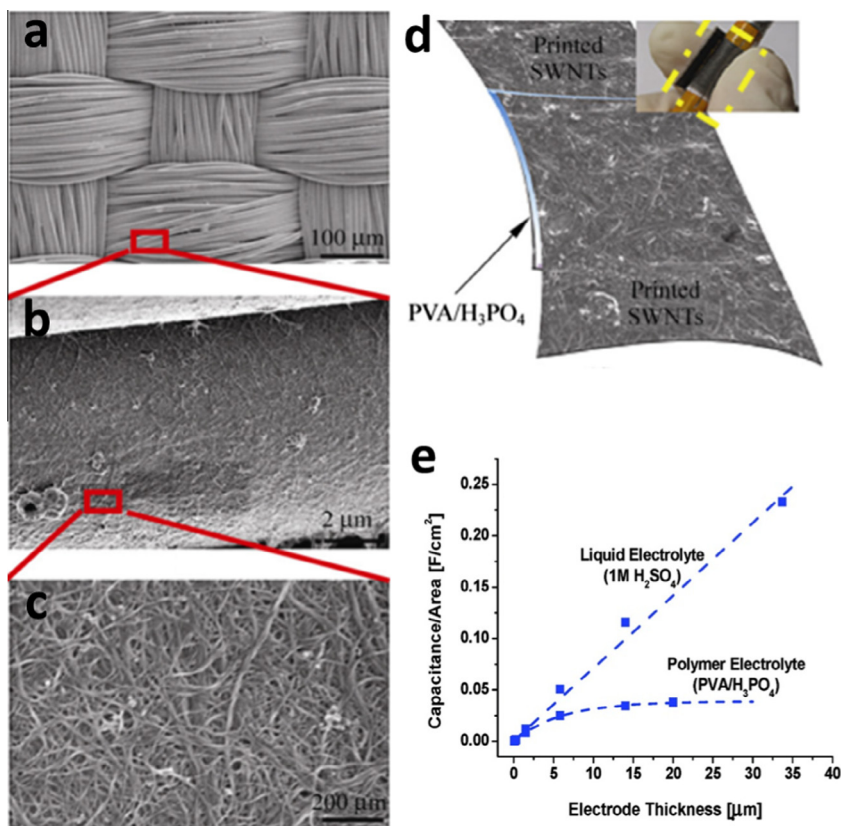


Fig. 11 – Inkjet-printed SWCNT supercapacitor on cloth fabric. (a)–(c) SEM images showing the uniform CNT coating on cloth fibers. (d) Schematic diagram of the inkjet-printed SC with electrolyte. Inset shows flexible SC wrapped around a pencil. Reprinted with permission from [9]. Copyright 2010 Springer. (e) Plot showing the thickness dependence of capacitance for a SC with printed CNT electrodes. (e) Reprinted with permission from [11]. Copyright 2009 American Chemical Society. (A color version of this figure can be viewed online.)

the opposite side of the paper. Then the SWCNTs dispersed in water with 1% sodium dodecylbenzenesulfonate were printed on both sides of the treated paper. The high wettability of the paper resulted in defect-free and high resolution printed patterns. Here, the CNTs acted as both the SC electrode material as well as the current collectors. These printed SCs exhibited a specific capacitance of 33 F/g at a specific power of 250,000 W/kg. This scalable fabrication technique using simple and commercially available materials could potentially be used to produce fully paper-based electronics.

Kaempgen et al. [11] used another method to fabricate CNT SC electrodes, by spraying a dispersion of SWCNTs in water onto PET substrates with the use of a tip sonicator. This created a tangled network of CNTs when the water evaporated, producing a highly conductive film. A gel electrolyte was sandwiched between two of these electrodes to construct a completed flexible device. The SCs fabricated by this printing method exhibited a higher specific capacitance (120 F/g) than those using thicker free-standing SWCNT films (80 F/g). This was due to greater wetting of the printed films and therefore a higher effective surface area. Additionally, the areal capacitance was directly related to the thickness of the electrode (Fig. 11e); a thicker film resulted in increased capacitance. The more viscous gel polymer electrolyte was

unable to penetrate as deep into the thicker films as the liquid electrolyte, resulting in a maximum capacitance when the electrode was approximately 20 μm thick. On the other hand, the relationship between thickness and capacitance linearly increased when using a liquid electrolyte, demonstrating that the capacitance can be finely tuned by controlling the electrode thickness.

Graphene has also been used as a printed SC electrode material [142,150] and has some advantages in terms of printing compared to CNTs. It can be printed in its oxidized form, GO, and subsequently reduced, allowing for higher concentration inks. This avoids the need for surfactants or functional groups, which increase contact resistance, as in the printed CNT electrodes. Additionally, by printing porous graphene [201,202], it may be possible to significantly increase the surface area and capacitance of printed SCs.

Printing carbon nanomaterials is becoming an increasingly popular method to fabricate SC electrodes. Porous CNT networks are ideal for SC electrodes due to their high electrical conductivities and surface areas, which improves the penetration of the electrolyte. Printing techniques enable tight control over the electrode thickness, which allows for fine tuning of the capacitance. They can also be used to deposit electrode materials on a variety of flexible substrates,

including clothing fibers and paper. Large-scale manufacturing of CNT SC electrodes by inkjet and roll-to-roll [8] printing processes may soon be realized.

4.3. Fuel cells

Fuel cells are electrochemical devices that directly convert electrochemical energy into electrical energy. Polymer electrolyte membrane fuel cells (PEMFCs) are promising alternative power sources for transportation and portable applications due to their high efficiency, near room temperature operation, and zero emissions. However, high cost is one of the main challenges facing the commercialization of PEMFCs. One of the primary cost-drivers is the membrane electrode assembly (MEA), which consists of the catalyst, electrolyte membrane, and gas diffusion layers (GDLs). Improving performance and reducing PEMFC cost requires efficient utilization of the catalyst and optimizing the structure of the MEA, which requires improving the design of the system architecture.

Catalyst layers (CL) are either applied to the gas diffusion layer, to produce a gas diffusion electrode (GDE), or applied to the membrane, to make a catalyst coated membrane (CCM). The CCM was pioneered in 1992 [203,204] and has become an industry standard due to its good performance, which arises from improved contact and bonding between the PEM and CL. Existing methods for depositing CLs include hand painting, decal transfer, spray coating, screen printing, and inkjet printing [122]. While spray coating has been widely used, screen and inkjet printing have gained attention as a result of their uniformity, patternability, and material usage. Another advantage of screen and inkjet printing is the ability to produce very thin CLs which increases the performance of the MEA.

As stated earlier in this review, printing processes depend strongly on the properties of the ink. FC catalysts are first dispersed in inks before being deposited. A FC catalyst ink is typically composed of several components including the Pt/carbon catalyst and ionomer dispersed in an aqueous solution [205]. Some mixture of low surface tension solvent such as isopropyl alcohol or ethanol is used to decrease the total ink surface tension and increase its volatility. Additionally, ethylene glycol or glycerol is sometimes used to adjust the viscosity and to act as a humectant to control drying [134].

Although it does not offer the same patternability as inkjet printing, screen printing can be done quickly and is easily scaled up. A single-step screen printing process may be used to coat the PEM or GDL with catalyst, though an optimal surface tension is needed. One group showed the effects of adjusting the ink surface tension when printing onto the GDL [134]. Their results point to improved adhesion of the CL and improved power density when using ink with a lower surface tension than the GDL substrate, compared to ink with surface tension higher than the substrate. The surface tension adjustment resulted in a more homogenous CL and improved the integrity of the MEA.

Taylor [125] and Towne [126] were among the first to report inkjet printing of CCMs and demonstrate the ultra-low Pt loadings that can be achieved with this technique. Taylor and colleagues used a variety of commercially available

carbon blacks, including Johnson Matthey's HiSPEC, as well as XC-72R, Monach 700, and Black Pearls 2000 (all from Cabot). They showed that MEAs with anodes prepared by inkjet printing had better performance than hand-painted anode CLs. Towne, meanwhile, reported that the power densities of printed MEAs were not as high as for a commercial MEA. However, it was shown that both thermal and piezo printers could be used to prepare CLs and that the resilience of the CCM to mechanical and chemical stresses was good, suggesting that printing could be a viable process for facile preparation of CCMs.

Thickness and uniformity of the layer can be controlled due to the ultra-small droplet sizes which are typically several picoliters in volume. CL thickness strongly affects FC performance as mass transport can be inhibited with excessive thickness. Shukla et al. [132] showed the dependence of thickness by creating CLs with an increasing number of printed layers. Results show that a thicker CL improves the ORR performance in the kinetic region due to the increased Pt content. However as the CL gets too thick there is a drop in the limiting current density in the mass transport region. The uniformity of a printed CL and spray coated CL can be seen in Fig. 12. The catalyst layer appears bright compared to the membrane. In the piezo-printed sample the CL is highly uniform and has a thickness of 5 μm , corresponding to 10 printed layers. The spray coated CL is considerably thicker and the lack of homogeneity is obvious from the sample image.

Inkjet printing can offer good patternability for creating unique CL shapes and forms. For instance, the catalyst density can be patterned to follow the flow channels of the bipolar plate, ensuring efficient use of the material in areas with a high concentration of reactant gases. Recently, Malevich et al. [131] demonstrated the use of patterned CCMs using piezo-inkjet printing. Their results point to the difficulty that remains in generating truly sharp features on patterned CCMs. Some work is still needed to achieve the resolution seen with more conventional substrates. Fine tuning of the ink properties with respect to the PEM may be necessary.

Perhaps the most important advantage of printing for FC catalysts is that it can lead to efficient utilization of the expensive catalyst material. With the high cost of Pt, it is desirable to ensure that its electro-catalytic surface is fully utilized. Thin CCMs fabricated by piezo-inkjet printing can achieve Pt utilizations of 100%, compared to utilization of 66% for CCMs prepared by spray coating [130]. A gradient structure can also be created that increases the Pt content near the PEM compared to the GDL side [125]. Fig. 12c and d shows the performance of printed CCMs with a varying number of layers compared to a spray coated CCM and a commercial CCM. It is clear that the overall performance of the commercial CCM is the highest and that performance decreases with a decreasing number of printed layers. This is due to the total Pt loading decreasing with the number of printed layers. However, Fig. 12d shows that the mass-specific power density is considerably higher for printed CCMs compared to the spray coated and commercial CCMs. This points to more efficient utilization of the Pt. The CCM with just two printed layers (cathode loading 0.02 mg Pt/cm²) showed nearly 7 times higher mass-specific power density than a commercial CCM (cathode loading 0.3 mg Pt/cm²)

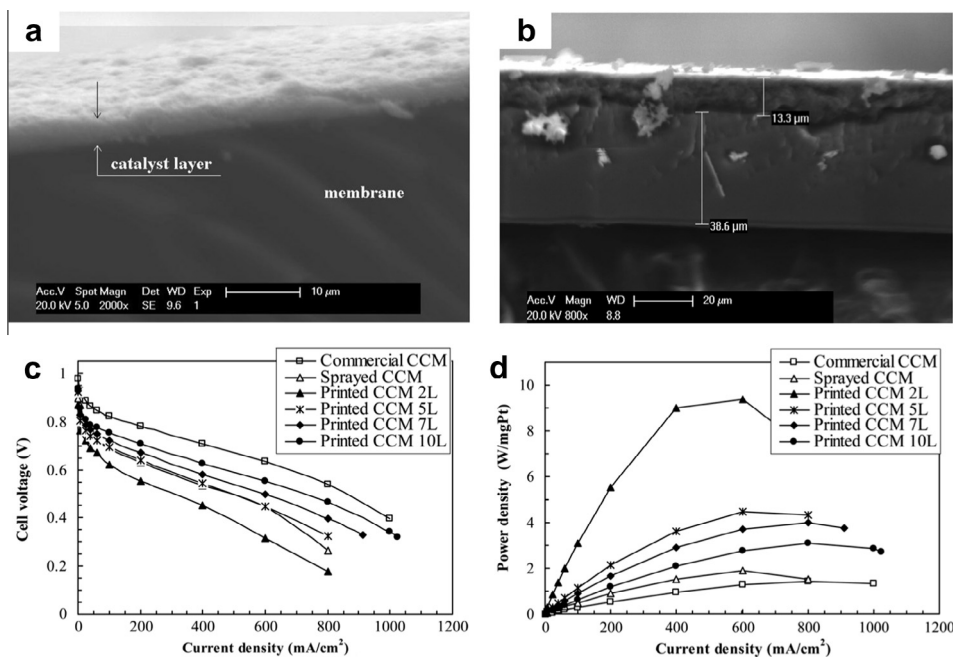


Fig. 12 – SEM images of CCMs prepared by (a) piezo-inkjet printing and (b) spray coating. The CL prepared by printing is the result of 10 printed layers, totalling 5 μm thick. (c, d) Performance of single cell tests of CCMs with cathodes prepared by piezo-inkjet printing and spray coating compared to a commercial CCM. Single cell tests were performed using H_2 and air at 60 $^\circ\text{C}$. Reprinted with permission from [130]. Copyright 2011 The Electrochemical Society.

[130]. Compared to a spray-coated CCM, the mass activity of an inkjet-printed CCM was 3.5 times higher at 850 mV.

The optimization of water management in the MEA is also a key issue to improve the performance of PEMFCs. The CL in an MEA fabricated by a screen printing method onto the GDL showed uniformly dispersed pores for maximum mass transport compared with a spray coating method [206]. This CL on a micro-porous layer resulted in lower ohmic resistance and low mass transport resistance due to enhanced adhesion between CL and membrane, and improved mass transport of fuel and vapors. In another study, a GDE prepared by a screen printing method also showed lower diffusion losses compared with other methods since a better distribution of pores by the screen printing method enhanced separation of the liquid and gas phase [207].

More research is needed in the field of printing for FCs. The rise of 3D printing may open doors to more integrated manufacturing of MEAs and other FC components. In the near-future, printing of nano-carbon materials may be coupled with other advanced deposition techniques to optimize the structure of the MEA to improve its water management and catalyst utilization. For instance, atomic layer deposition (ALD) [208,209] may be used to deposit Pt on a printed carbon support layer. ALD relies on active surface species to chemically deposit material and can have area-selectivity that may complement the printing techniques currently used. This has potential to increase the Pt utilization because the Pt catalyst can be deposited only where needed. Also, this can be used to increase the Pt content at the surface of the CL closest to the membrane. For large scale production of MEAs, printing speeds would likely have to increase to compete with current manufacturing technologies.

4.4. Solar cells

As concerns about pollution and global warming rise, there is a growing demand to shift away from fossil fuels in favor of renewable energy sources. Wind, solar, geothermal, biomass, and hydroelectric energy have all been studied extensively for their potential as replacements to the traditionally used coal, natural gas, and petroleum. Of these, solar has the highest potential annual energy harvest [210]. However, the low energy conversion efficiencies and high costs of today's photovoltaic cells limit their use to less than 1% of global energy consumption [211].

Solar cells absorb photons and convert their energy into electrical energy. When a photon is absorbed, an electron-hole pair is created in the semiconducting material of the cell via the photoelectric effect. The main distinguishing feature between organic and inorganic cells is the localization of this electron-hole pair. In organic photovoltaics (OPVs), the electron-hole pair is confined to a region of only a few cubic nanometers, making recombination a common issue [212]. Bulk heterojunctions (BHJs) mitigate this problem by dispersing an electron acceptor into the semiconductor matrix, such as fullerene. When an electron-hole pair is created, the electron is attracted to a nearby fullerene molecule. These electron-hole pairs can then be separated and travel toward the cell electrodes. Once the electrons are collected, the electrical current can be used to power an external load.

OPVs have recently been gaining attention as potential candidates for next-generation solar cells due to their high absorption coefficients, low cost, scalability, and the ability to fabricate them on flexible substrates. The BHJ configuration has been improved over the past decade and power

conversion efficiencies of 10% have been recorded. By using high throughput processing methods, such as coating and printing techniques, it is predicted that the cost of these OPVs can be reduced to make them competitive with other energy sources [213].

Polymer:fullerene blends are the most commonly studied materials for BHJs [214]. They are composed of functionalized fullerenes (almost exclusively PCBM) dispersed in a semiconducting polymer (usually P3HT). Solution processing techniques, including casting, spin coating, blade coating, screen printing, inkjet printing, and roll-to-roll processing, are most common for fabricating these types of devices.

The first reported screen printed polymer:fullerene blend for OPVs was reported by Shaheen et al. in 2001 and achieved a power conversion efficiency of 4.3% [38]. Since then, few studies using screen printing for polymer:fullerene cells have been reported [35,76,77], due to the high viscosity and low volatility requirements for screen printing inks. Most P3HT:PCBM solutions are low viscosity mixtures in dichlorobenzene, a highly volatile solvent, which results in the ink running through the screen and drying out too quickly [215]. For this reason, Jørgensen et al. [215] developed various thermo-cleavable solvent systems with increased viscosity and stability at room temperature.

A simpler alternative to this, however, is to use inkjet printing, which demands low viscosity and quick-drying solvents. A number of studies have reported using inkjet printing for fabricating polymer:fullerene active layers in photovoltaic devices [13,15,72,73,138–140]. Hoth et al. [13] experimented with different solvents for dispersing P3HT:PCBM and concluded that a mixture of two organic solvents with varying surface tensions and volatilities achieved optimal jetting properties. The lower surface tension and more volatile solvent (mesitylene) improved the wettability of the ink on the substrate, while the higher surface tension and lower volatility solvent (oDCB) was used to prevent gelation that leads to nozzle clogging. A more extensive combinatorial study showed similar results [72]. In addition, Neophytou et al. [73] optimized and compared three different coating techniques for preparing organic solar cells: inkjet printing, doctor blading, and spin coating. They found that inkjet printing resulted in the lowest power conversion efficiency (3.07%), while doctor blading exhibited the highest (3.58%). This was attributed to small differences in thickness and morphology of the inkjet printed films, due to the limited processing parameters and physical properties of the ink. The lower performance of the printed OPV active layers compared to other fabrication techniques may be acceptable if the costs of large-scale production are sufficiently reduced by printing.

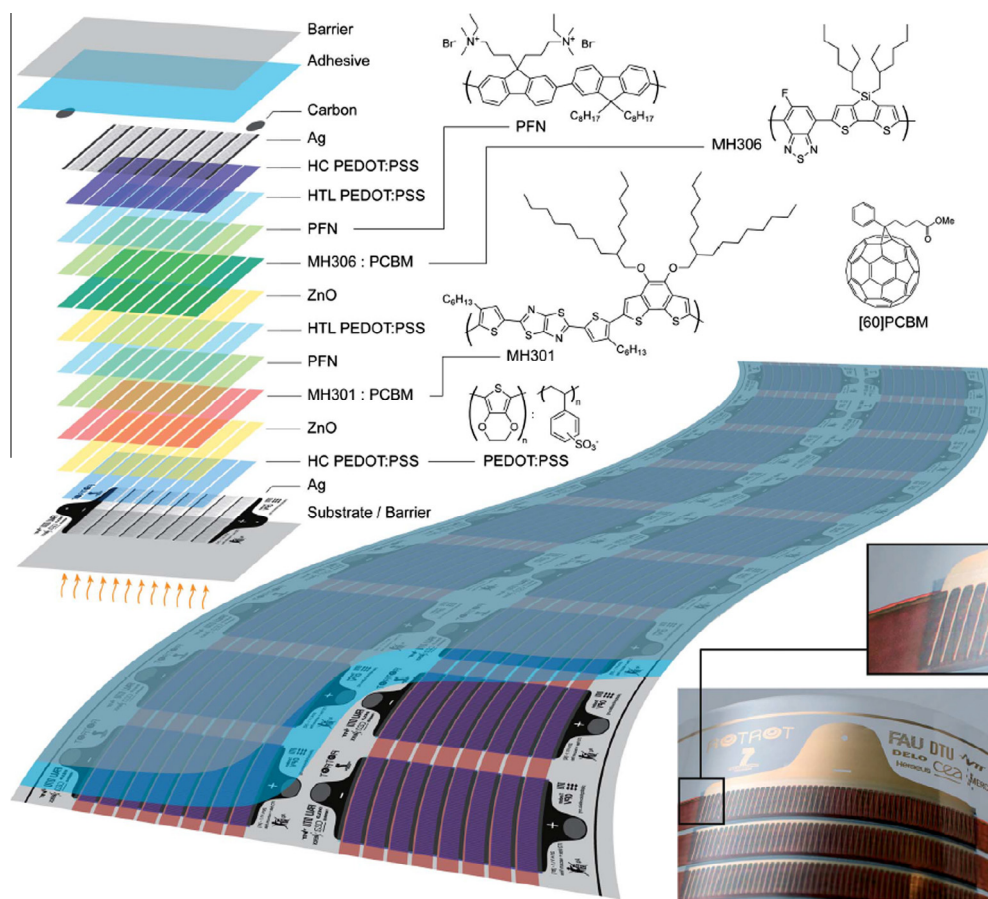


Fig. 13 – Illustrations and photographs of a printed 14-layer tandem stack solar cell. Each layer was fabricated by a roll-to-roll solution processing method, including screen printing, flexographic printing, and slot-die coating. Reprinted with permission from [232]. Copyright 2014 The Royal Society of Chemistry. (A color version of this figure can be viewed online.)

The transparent electrode in nearly all the examples of printed polymer:fullerene blends for OPVs is composed of indium tin oxide (ITO) due to its high electrical conductivity, optical transparency, and ease of processing into thin films. However, there is a recent trend to move away from ITO, as it is limited by its mechanical brittleness [216], contamination via ion diffusion [217], and low earth abundance. Graphene and CNTs are ideally suited to replace ITO as the transparent electrode in OPVs, as they exhibit high conductivity, robust mechanical properties, relatively lower costs, optical transparency, and comparable efficiencies [80,218–220]. Additionally, as we have seen, they can be easily deposited as thin films on any substrate using printing techniques. Recently, intensive research has focused on large-area production based on roll-to-roll processing and printing techniques [221–226]. By printing graphene and CNTs, researchers have developed solar cells with short-circuit current densities [227,228], power conversion efficiencies [228,229], and efficient hole transport layers [229,230], comparable to traditional photovoltaic devices.

Choi et al. [231] used a typical transfer printing process for graphene to fabricate a transparent OPV electrode. First, graphene was grown on a copper foil via chemical vapor deposition. Poly(methyl methacrylate) (PMMA) was then spin-coated on top of the graphene film and the copper was etched away. The graphene/PMMA was then transferred onto a glass substrate and the PMMA layer was subsequently dissolved with acetone, leaving a multi-layered sheet of graphene remaining on the glass. The remainder of the solar cell was then assembled on top of this transparent electrode. The completed solar cell exhibited a power conversion efficiency of 1.17%, which was about half that of the reference cell using an ITO electrode. The low performance was attributed to the higher

sheet resistance of the graphene electrode, caused by residual PMMA and wrinkles in the graphene layers. The authors suggest that with optimization of the transfer printing process, the performance of these solar cells could be improved.

It is evident from these examples that improvements to the printing processes must be made before they can be used for industrial solar cell fabrication. Solution processing offers a cheap, scalable method of fabricating entire solar cells. Andersen et al. [232] developed an impressive roll-to-roll process using various solution processing methods to produce 14-layer flexible polymer solar cells (Fig. 13). Each layer was deposited with a rotary printing or coating technique. For example, the carbon contacts were screen printed and the absorber PCBM layers were slot-die coated. Continuous printing and coating techniques like these are the future of industrial-scale OPV manufacturing, as they allow for low-cost [233], reliable fabrication of these devices.

In addition, combining polymer:fullerene blend printing techniques with graphene transparent electrode replacements for ITO may lead to economically viable solar cells in the future. The high cost of fullerenes is currently a limiting factor for the large-scale production of polymer:fullerene solar cells. Driving down the cost of these devices may ultimately lead to the widespread adoption of this promising renewable energy conversion technology.

5. Summary and perspectives

Printing technology has been widely used in both academic laboratories and industry for many applications. Printing carbon nanomaterials in particular has made possible significant advances for energy applications, as summarized in Fig. 14. A growing trend toward using printing techniques for energy

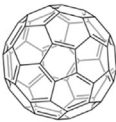
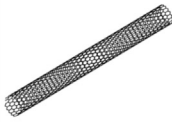
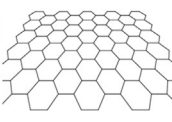
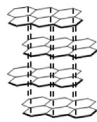


































	Fullerenes	Carbon Nanotubes	Graphene	Other Carbons
				
Batteries		  	  	  
Supercapacitors		   	   	  
Fuel Cells		 	 	  
Solar Cells	 	 	  	

Fig. 14 – Summary of the current state of printed nanomaterials for energy storage and conversion applications. Each symbol represents a printing technique that has been used and reported for the given application and nanomaterial. A dashed circle indicates that that printing technique has not yet been used for the corresponding application and nanomaterial, but is a good candidate for future research.

device fabrication is expected. Printing of nanostructured carbons enables inexpensive, large-scale assembly with precise control over thickness and patternability. Applied to the field of energy storage and conversion, printing techniques for depositing graphene and CNTs should effectively improve production rates and increase the efficiency of material utilization.

Nevertheless, despite the rapidly growing number of publications on printing carbon nanomaterials in the field of energy storage and conversion, their industrial-level applications are still limited today. This should be mainly attributed not only to the fact that these materials are relatively new but also to the fact that necessary processing parameters have not yet fully matured. In particular, a number of key issues must be overcome to improve the formulations of nanostructured carbon inks before their full potential can be realized, including stability in solution, uniform particle size distribution, and the ability to form stable dispersions without compromising electronic conductivity.

Particularly for inkjet printing, a number of studies have attempted to address these problems by functionalizing nanostructured carbons with covalently-bonded molecules, adding surfactants to the aqueous solutions, and oxidizing their surfaces to make them more readily-dispersed in polar solvents. Considerable progress has been made toward realizing high conductivity printed graphene and CNT films, but challenges still exist, especially with contact resistance between particles. One possible solution may be to print doped carbon nanomaterials, which can be more easily dispersed in water and exhibit even higher conductivities than their pristine counterparts. Both nitrogen-doped graphene and nitrogen-doped CNTs have shown improved performance for energy storage devices. Logically, the next step will be to develop printing techniques to deposit these materials for use in functional devices.

3D printing may also be a promising alternative to the more common inkjet, screen, and transfer printing techniques. By adopting 3D printing technology, various 3D-structured designs of electrodes can be realized in a highly repeatable way, which is greatly favored in the area of mass production of high performance energy storage and conversion devices. For example, a 3D-structured Li-ion battery can exhibit much higher energy and power densities than that of conventional planar design. A 3D structured electrode possesses much higher surface area and can be greatly favored for both metal-air batteries and electrochemical capacitors. Though 3D printing is making strides in other industrial fields, it remains an unproven process for fabricating energy devices. Nevertheless, as functional inks containing carbon nanomaterials are further developed and 3D printers are improved, we can expect to see a translation of this technology from laboratory to industry. This will ultimately result in affordable, high performance devices.

Overall, printing is not meant as a replacement for high precision fabrication techniques, but instead provides a great opportunity to produce high volumes of large area devices at low cost. In the context of the green, renewable energy devices discussed in this review, printing carbon nanomaterials may lead to simplified manufacturing and improved cost effectiveness. Traditional production processes can improve

and evolve by adopting printing systems that allow for more robust, customizable, waste-free, and lean additive manufacturing techniques. The combination of printing technology and carbon nanomaterials will result in a diverse range of applications in the field of energy storage and conversion, calling for tremendous research efforts now and in the future.

Acknowledgments

This work was supported by the Natural Sciences and Engineering Research Council of Canada (NSERC), Canada Research Chair (CRC) Program, Canada Foundation for Innovation (CFI), Ontario Research Fund (ORF), and University of Western Ontario. Stephen Lawes and Adam Riese also acknowledge the Province of Ontario and the University of Western Ontario for the Queen Elizabeth II Graduate Scholarship in Science and Technology.

REFERENCES

- [1] Xu F, Wang T, Li W, Jiang Z. Preparing ultra-thin nano-MnO₂ electrodes using computer jet-printing method. *Chem Phys Lett* 2003;375(1-2):247–51.
- [2] Zhao Y, Zhou Q, Liu L, Xu J, Yan M, Jiang Z. A novel and facile route of ink-jet printing to thin film SnO₂ anode for rechargeable lithium ion batteries. *Electrochim Acta* 2006;51(13):2639–45.
- [3] Huang J, Yang J, Li W, Cai W, Jiang Z. Electrochemical properties of LiCoO₂ thin film electrode prepared by ink-jet printing technique. *Thin Solid Films* 2008;516(10):3314–9.
- [4] Zhao Y, Liu G, Liu L, Jiang Z. High-performance thin-film Li₄Ti₅O₁₂ electrodes fabricated by using ink-jet printing technique and their electrochemical properties. *J Solid State Electrochem* 2008;13(5):705–11.
- [5] Hilder M, Winther-Jensen B, Clark NB. Paper-based, printed zinc-air battery. *J Power Sources* 2009;194(2):1135–41.
- [6] Lee J-H, Wee S-B, Kwon M-S, Kim H-H, Choi J-M, Song MS, et al. Strategic dispersion of carbon black and its application to ink-jet-printed lithium cobalt oxide electrodes for lithium ion batteries. *J Power Sources* 2011;196(15):6449–55.
- [7] Zhao C, Wang C, Gorkin R, Beirne S, Shu K, Wallace GG. Three dimensional (3D) printed electrodes for interdigitated supercapacitors. *Electrochem Commun* 2014;41:20–3.
- [8] Arcila-Velez MR, Zhu J, Childress A, Karakaya M, Podila R, Rao AM, et al. Roll-to-roll synthesis of vertically aligned carbon nanotube electrodes for electrical double layer capacitors. *Nano Energy* 2014;8:9–16.
- [9] Chen P, Chen H, Qiu J, Zhou C. Inkjet printing of single-walled carbon nanotube/RuO₂ nanowire supercapacitors on cloth fabrics and flexible substrates. *Nano Res* 2010;3(8):594–603.
- [10] Pech D, Brunet M, Taberna P-L, Simon P, Fabre N, Mesnilgrente F, et al. Elaboration of a microstructured inkjet-printed carbon electrochemical capacitor. *J Power Sources* 2010;195(4):1266–9.
- [11] Kaempgen M, Chan CK, Ma J, Cui Y, Gruner G. Printable thin film supercapacitors using single-walled carbon nanotubes. *Nano Lett* 2009;9(5):1872–6.
- [12] Krebs FC. Fabrication and processing of polymer solar cells: A review of printing and coating techniques. *Sol Energy Mater Sol Cells* 2009;93(4):394–412.

- [13] Hoth CN, Choulis SA, Schilinsky P, Brabec CJ. High photovoltaic performance of inkjet printed polymer: fullerene blends. *Adv Mater* 2007;19(22):3973–8.
- [14] Kim HS, Kang JS, Park JS, Hahn HT, Jung HC, Joung JW. Inkjet printed electronics for multifunctional composite structure. *Compos Sci Technol* 2009;69(7–8):1256–64.
- [15] Hoth CN, Schilinsky P, Choulis SA, Brabec CJ. Printing highly efficient organic solar cells. *Nano Lett* 2008;8(9):2806–13.
- [16] Steirer KX, Berry JJ, Reese MO, van Hest MFAM, Miedaner A, Liberatore MW, et al. Ultrasonically sprayed and inkjet printed thin film electrodes for organic solar cells. *Thin Solid Films* 2009;517(8):2781–6.
- [17] Aden J, Bohórquez J, Collins D, Crook M, García A, Hess U. The third-generation HP thermal inkjet printhead. *Hewlett-Packard J* 1994:41–5.
- [18] Li J, Ye F, Vaziri S, Muhammed M, Lemme MC, Östling M. Efficient inkjet printing of graphene. *Adv Mater* 2013;25(29):3985–92.
- [19] Stringer J, Derby B. Limits to feature size and resolution in ink jet printing. *J Eur Ceram Soc* 2009;29(5):913–8.
- [20] Lim JA, Cho JH, Jang Y, Han JT, Cho K. Precise control of surface wettability of mixed monolayers using a simple wiping method. *Thin Solid Films* 2006;515(4):2079–84.
- [21] Deegan RD, Bakajin O, Dupont TF, Huber G, Nagel SR, Witten TA. Capillary flow as the cause of ring stains from dried liquid drops. *Nature* 1997;389(6653):827–9.
- [22] Soltman D, Subramanian V. Inkjet-printed line morphologies and temperature control of the coffee ring effect. *Langmuir* 2008;24(5):2224–31.
- [23] Deegan RD, Bakajin O, Dupont TF, Huber G, Nagel SR, Witten TA. Contact line deposits in an evaporating drop. *Phys Rev E* 2000;62(1):756–65.
- [24] Kim D, Jeong S, Park BK, Moon J. Direct writing of silver conductive patterns: improvement of film morphology and conductance by controlling solvent compositions. *Appl Phys Lett* 2006;89(26):264101.
- [25] Park J, Moon J. Control of colloidal particle deposit patterns within picoliter droplets ejected by ink-jet printing. *Langmuir* 2006;22(8):3506–13.
- [26] de Gans B-J, Schubert US. Inkjet printing of well-defined polymer dots and arrays. *Langmuir* 2004;20(18):7789–93.
- [27] Derby B. Inkjet printing of functional and structural materials: fluid property requirements, feature stability, and resolution. *Annu Rev Mater Res* 2010;40(1):395–414.
- [28] Cummins G, Desmulliez MPY. Inkjet printing of conductive materials: a review. *Circuit World* 2012;38(4):193–213.
- [29] Su Y, Du J, Sun D, Liu C, Cheng H. Reduced graphene oxide with a highly restored π -conjugated structure for inkjet printing and its use in all-carbon transistors. *Nano Res* 2013;6(11):842–52.
- [30] Schiaffino S, Sonin AA. Molten droplet deposition and solidification at low Weber numbers. *Phys Fluids* 1997;9(11):3172–87.
- [31] Bao Z, Feng Y, Dodabalapur A, Raju VR, Lovinger AJ. High-performance plastic transistors fabricated by printing techniques. *Chem Mater* 1997;9(6):1299–301.
- [32] Rogers JA, Bao Z, Raju VR. Nonphotolithographic fabrication of organic transistors with micron feature sizes. *Appl Phys Lett* 1998;72(21):2716–8.
- [33] Park M-S, Hyun S-H, Nam S-C. Mechanical and electrical properties of a LiCoO₂ cathode prepared by screen-printing for a lithium-ion micro-battery. *Electrochim Acta* 2007;52(28):7895–902.
- [34] Ohta S, Komagata S, Seki J, Saeki T, Morishita S, Asaoka T. All-solid-state lithium ion battery using garnet-type oxide and Li₃BO₃ solid electrolytes fabricated by screen-printing. *J Power Sources* 2013;238:53–6.
- [35] Krebs FC, Jørgensen M, Norrman K, Hagemann O, Alstrup J, Nielsen TD, et al. A complete process for production of flexible large area polymer solar cells entirely using screen printing—first public demonstration. *Sol Energy Mater Sol Cells* 2009;93(4):422–41.
- [36] Krebs FC. Polymer solar cell modules prepared using roll-to-roll methods: knife-over-edge coating, slot-die coating and screen printing. *Sol Energy Mater Sol Cells* 2009;93(4):465–75.
- [37] Ito S, Chen P, Comte P, Nazeeruddin MK, Liska P, Péchy P, et al. Fabrication of screen-printing pastes from TiO₂ powders for dye-sensitized solar cells. *Prog Photovoltaics* 2007;15(7):603–12.
- [38] Shaheen SE, Radspinner R, Peyghambarian N, Jabbour GE. Fabrication of bulk heterojunction plastic solar cells by screen printing. *Appl Phys Lett* 2001;79(18):2996–8.
- [39] Somalu MR, Yufit V, Shapiro IP, Xiao P, Brandon NP. The impact of ink rheology on the properties of screen-printed solid oxide fuel cell anodes. *Int J Hydrogen Energy* 2013;38(16):6789–801.
- [40] Von Dollen P, Barnett S. A study of screen printed yttria-stabilized zirconia layers for solid oxide fuel cells. *J Am Ceram Soc* 2005;88(12):3361–8.
- [41] Somalu MR, Brandon NP. Rheological studies of nickel/Scandia-stabilized-zirconia screen printing inks for solid oxide fuel cell anode fabrication. *J Am Ceram Soc* 2012;95(4):1220–8.
- [42] Sung JH, Lee JY, Kim S, Suh J, Kim J, Ahn KH, et al. Effect of particle size in Ni screen printing paste of incompatible polymer binders. *J Mater Sci* 2010;45(9):2466–73.
- [43] Ried P, Lorenz C, Brönstrup A, Graule T, Menzler NH, Sitte W, et al. Processing of YSZ screen printing pastes and the characterization of the electrolyte layers for anode supported SOFC. *J Eur Ceram Soc* 2008;28(9):1801–8.
- [44] Phair JW. Rheological analysis of concentrated zirconia pastes with ethyl cellulose for screen printing SOFC electrolyte films. *J Am Ceram Soc* 2008;91(7):2130–7.
- [45] Li H, Xie Z, Zhang Y, Wang J. The effects of ethyl cellulose on PV performance of DSSC made of nanostructured ZnO pastes. *Thin Solid Films* 2010;518(24, Supplement):e68–71.
- [46] Chen JH, Ishigami M, Jang C, Hines DR, Fuhrer MS, Williams ED. Printed Graphene Circuits. *Adv Mater* 2007;19(21):3623–7.
- [47] Hines DR, Mezhenny S, Breban M, Williams ED, Ballarotto VW, Esen G, et al. Nanotransfer printing of organic and carbon nanotube thin-film transistors on plastic substrates. *Appl Phys Lett* 2005;86(16):163101.
- [48] Kim T-H, Cho K-S, Lee EK, Lee SJ, Chae J, Kim JW, et al. Full-colour quantum dot displays fabricated by transfer printing. *Nat Photon* 2011;5(3):176–82.
- [49] Cerf A, Alava T, Barton RA, Craighead HG. Transfer-printing of single DNA molecule arrays on graphene for high-resolution electron imaging and analysis. *Nano Lett* 2011;11(10):4232–8.
- [50] Mizuno H, Kaneko T, Sakata I, Matsubara K. Capturing by self-assembled block copolymer thin films: transfer printing of metal nanostructures on textured surfaces. *Chem Commun* 2014;50(3):362–4.
- [51] Hyun WJ, Secor EB, Hersam MC, Frisbie CD, Francis LF. High-resolution patterning of graphene by screen printing with a silicon stencil for highly flexible printed electronics. *Adv Mater* 2015;27(1):109–15.
- [52] Loo Y-L, Hsu JWP, Willett RL, Baldwin KW, West KW, Rogers JA. High-resolution transfer printing on GaAs surfaces using alkane dithiol monolayers. *J Vac Sci Technol B* 2002;20(6):2853–6.
- [53] Jeong JW, Yang SR, Hur YH, Kim SW, Baek KM, Yim S, et al. High-resolution nanotransfer printing applicable to diverse

- surfaces via interface-targeted adhesion switching. *Nat Commun* 2014;5.
- [54] Hines DR, Ballarotto VW, Williams ED, Shao Y, Solin SA. Transfer printing methods for the fabrication of flexible organic electronics. *J Appl Phys* 2007;101(2):024503.
- [55] Sun K, Wei TS, Ahn BY, Seo JY, Dillon SJ, Lewis JA. 3D printing of interdigitated Li-ion microbattery architectures. *Adv Mater* 2013;25(33):4539–43.
- [56] Zhao C, Wang C, Gorkin Iii R, Beirne S, Shu K, Wallace GG. Three dimensional (3D) printed electrodes for interdigitated supercapacitors. *Electrochem Commun* 2014;41(0):20–3.
- [57] Bose S, Vahabzadeh S, Bandyopadhyay A. Bone tissue engineering using 3D printing. *Mater Today* 2013;16(12):496–504.
- [58] Muth JT, Vogt DM, Truby RL, Mengüç Y, Kolesky DB, Wood RJ, et al. Embedded 3D printing of strain sensors within highly stretchable elastomers. *Adv Mater* 2014;26(36):6307–12.
- [59] Kim JH, Chang WS, Kim D, Yang JR, Han JT, Lee G-W, et al. 3D printing of reduced graphene oxide nanowires. *Adv Mater* 2015;27(1):157–61.
- [60] Kelsall RW. Hybrid silicon lasers: rubber stamp for silicon photonics. *Nat Photon* 2012;6(9):577–9.
- [61] Han Y, Wei C, Dong J. Super-resolution electrohydrodynamic (EHD) 3D printing of micro-structures using phase-change inks. *Manufact Lett* 2014;2(4):96–9.
- [62] Goldie DM, Hourd AC, Harvie MR, Thomson J, Abdolvand A. Scatter-limited conduction in printed platinum nanofilms. *J Mater Sci* 2015;50(3):1169–74.
- [63] Bae S, Kim H, Lee Y, Xu X, Park J-S, Zheng Y, et al. Roll-to-roll production of 30-inch graphene films for transparent electrodes. *Nat Nanotechnol* 2010;5(8):574–8.
- [64] Kim T-i, Kim MJ, Jung YH, Jang H, Dagdeviren C, Pao HA, et al. Thin film receiver materials for deterministic assembly by transfer printing. *Chem Mater* 2014;26(11):3502–7.
- [65] Kroto HW, Heath JR, O'Brien SC, Curl RF, Smalley RE. C60: buckminsterfullerene. *Nature* 1985;318(6042):162–3.
- [66] Itami K. Molecular catalysis for fullerene functionalization. *Chem Rec* 2011;11(5):226–35.
- [67] Chen J, Tsekouras G, Officer DL, Wagner P, Wang CY, Too CO, et al. Novel fullerene-functionalised poly(terthiophenes). *J Electroanal Chem* 2007;599(1):79–84.
- [68] He C-L, Liu R, Li D-D, Zhu S-E, Wang G-W. Synthesis and functionalization of [60]fullerene-fused imidazolines. *Org Lett* 2013;15(7):1532–5.
- [69] Wallace GG, Chen J, Li D, Moulton SE, Razal JM. Nanostructured carbon electrodes. *J Mater Chem* 2010;20(18):3553–62.
- [70] Hummelen JC, Knight BW, LePeq F, Wudl F, Yao J, Wilkins CL. Preparation and characterization of fulleroid and methanofullerene derivatives. *J Org Chem* 1995;60(3):532–8.
- [71] Semenov KN, Charykov NA, Keskinov VA, Piartman AK, Blokhin AA, Kopyrin AA. Solubility of light fullerenes in organic solvents. *J Chem Eng Data* 2009;55(1):13–36.
- [72] Teichler A, Eckardt R, Hoepfner S, Friebe C, Perelaer J, Senes A, et al. Combinatorial screening of polymer: fullerene blends for organic solar cells by inkjet printing. *Adv Energy Mater* 2011;1(1):105–14.
- [73] Neophytou M, Cambarau W, Hermerschmidt F, Waldauf C, Christodoulou C, Pacios R, et al. Inkjet-printed polymer-fullerene blends for organic electronic applications. *Microelectron Eng* 2012;95:102–6.
- [74] Yan J, Saunders BR. Third-generation solar cells: a review and comparison of polymer:fullerene, hybrid polymer and perovskite solar cells. *R Soc Chem Adv* 2014;4(82):43286–314.
- [75] Ruoff RS, Tse DS, Malhotra R, Lorents DC. Solubility of fullerene (C60) in a variety of solvents. *J Phys Chem* 1993;97(13):3379–83.
- [76] Krebs FC, Alstrup J, Spanggaard H, Larsen K, Kold E. Production of large-area polymer solar cells by industrial silk screen printing, lifetime considerations and lamination with polyethyleneterephthalate. *Sol Energy Mater Sol Cells* 2004;83(2–3):293–300.
- [77] Bing Z, Heeyeop C, Sung Min C. Screen-printed polymer: fullerene bulk-heterojunction solar cells. *Jpn J Appl Phys* 2009;48(2R):020208.
- [78] Novoselov KS, Geim AK, Morozov SV, Jiang D, Zhang Y, Dubonos SV, et al. Electric field effect in atomically thin carbon films. *Science* 2004;306(5696):666–9.
- [79] Kyeong-Jae L, Chandrakasan AP, Kong J. Breakdown current density of CVD-grown multilayer graphene interconnects. *Electron Device Lett* 2011;32(4):557–9.
- [80] Zhang DW, Li XD, Li HB, Chen S, Sun Z, Yin XJ, et al. Graphene-based counter electrode for dye-sensitized solar cells. *Carbon* 2011;49(15):5382–8.
- [81] Pumera M. Electrochemistry of graphene: new horizons for sensing and energy storage. *Chem Rec* 2009;9(4):211–23.
- [82] Williams JW, Van Holde KE, Baldwin RL, Fujita H. The theory of sedimentation analysis. *Chem Rev* 1958;58(4):715–44.
- [83] Schuck P. Size-distribution analysis of macromolecules by sedimentation velocity ultracentrifugation and Lamm equation modeling. *Biophys J* 2000;78(3):1606–19.
- [84] Torrisi F, Hasan T, Wu W, Sun Z, Lombardo A, Kulmala TS, et al. Inkjet-printed graphene electronics. *ACS Nano* 2012;6(4):2992–3006.
- [85] Zacharia R, Ulbricht H, Hertel T. Interlayer cohesive energy of graphite from thermal desorption of polyaromatic hydrocarbons. *Phys Rev B* 2004;69(15).
- [86] Arapov K, Abbel R, de With G, Friedrich H. Inkjet printing of graphene. *Faraday Discuss* 2014;173:323–36.
- [87] Secor EB, Prabhumirashi PL, Puntambekar K, Geier ML, Hersam MC. Inkjet printing of high conductivity, flexible graphene patterns. *J Phys Chem Lett* 2013;4(8):1347–51.
- [88] Englert JM, Röhr J, Schmidt CD, Graupner R, Hundhausen M, Hauke F, et al. Soluble graphene: generation of aqueous graphene solutions aided by a perylenebisimide-based bolaamphiphile. *Adv Mater* 2009;21(42):4265–9.
- [89] Su Q, Pang S, Alijani V, Li C, Feng X, Müllen K. Composites of graphene with large aromatic molecules. *Adv Mater* 2009;21(31):3191–5.
- [90] Tasis D, Tagmatarchis N, Bianco A, Prato M. Chemistry of carbon nanotubes. *Chem Rev* 2006;106(3):1105–36.
- [91] Wei D, Li H, Han D, Zhang Q, Niu L, Yang H, et al. Properties of graphene inks stabilized by different functional groups. *Nanotechnology* 2011;22(24):245702.
- [92] Eda G, Fanchini G, Chhowalla M. Large-area ultrathin films of reduced graphene oxide as a transparent and flexible electronic material. *Nat Nanotechnol* 2008;3(5):270–4.
- [93] Gómez-Navarro C, Weitz RT, Bittner AM, Scolari M, Mews A, Burghard M, et al. Electronic transport properties of individual chemically reduced graphene oxide sheets. *Nano Lett* 2007;7(11):3499–503.
- [94] Mattevi C, Eda G, Agnoli S, Miller S, Mkhoyan KA, Celik O, et al. Evolution of electrical, chemical, and structural properties of transparent and conducting chemically derived graphene thin films. *Adv Funct Mater* 2009;19(16):2577–83.
- [95] Nirmalraj PN, Lutz T, Kumar S, Duesberg GS, Boland JJ. Nanoscale mapping of electrical resistivity and connectivity in graphene strips and networks. *Nano Lett* 2010;11(1):16–22.
- [96] Hallam T, Shakouri A, Poliani E, Rooney AP, Ivanov I, Potie A, et al. Controlled folding of graphene: GraFold printing. *Nano Lett* 2014.
- [97] Panchakarla LS, Subrahmanyam KS, Saha SK, Govindaraj A, Krishnamurthy HR, Waghmare UV, et al. Synthesis,

- structure, and properties of boron- and nitrogen-doped graphene. *Adv Mater* 2009;21(46):4726–30.
- [98] Qu L, Liu Y, Baek J-B, Dai L. Nitrogen-Doped Graphene as Efficient Metal-Free Electrocatalyst for Oxygen Reduction in Fuel Cells. *ACS Nano* 2010;4(3):1321–6.
- [99] Shao Y, Zhang S, Engelhard MH, Li G, Shao G, Wang Y, et al. Nitrogen-doped graphene and its electrochemical applications. *J Mater Chem* 2010;20(35):7491–6.
- [100] Reddy ALM, Srivastava A, Gowda SR, Gullapalli H, Dubey M, Ajayan PM. Synthesis of nitrogen-doped graphene films for lithium battery application. *ACS Nano* 2010;4(11):6337–42.
- [101] Wu Z-S, Ren W, Xu L, Li F, Cheng H-M. Doped graphene sheets as anode materials with superhigh rate and large capacity for lithium ion batteries. *ACS Nano* 2011;5(7):5463–71.
- [102] Li X, Geng D, Zhang Y, Meng X, Li R, Sun X. Superior cycle stability of nitrogen-doped graphene nanosheets as anodes for lithium ion batteries. *Electrochem Commun* 2011;13(8):822–5.
- [103] Jeong HM, Lee JW, Shin WH, Choi YJ, Shin HJ, Kang JK, et al. Nitrogen-doped graphene for high-performance ultracapacitors and the importance of nitrogen-doped sites at basal planes. *Nano Lett* 2011;11(6):2472–7.
- [104] Wu Z-S, Winter A, Chen L, Sun Y, Turchanin A, Feng X, et al. Three-dimensional nitrogen and boron co-doped graphene for high-performance all-solid-state supercapacitors. *Adv Mater* 2012;24(37):5130–5.
- [105] Wen Z, Wang X, Mao S, Bo Z, Kim H, Cui S, et al. Crumpled nitrogen-doped graphene nanosheets with ultrahigh pore volume for high-performance supercapacitor. *Adv Mater* 2012;24(41):5610–6.
- [106] Berber S, Kwon Y-K, Tománek D. Unusually high thermal conductivity of carbon nanotubes. *Phys Rev Lett* 2000;84(20):4613–6.
- [107] Troiani HE, Miki-Yoshida M, Camacho-Bragado GA, Marques MAL, Rubio A, Ascencio JA, et al. Direct observation of the mechanical properties of single-walled carbon nanotubes and their junctions at the atomic level. *Nano Lett* 2003;3(6):751–5.
- [108] Martel R, Schmidt T, Shea HR, Hertel T, Avouris P. Single- and multi-wall carbon nanotube field-effect transistors. *Appl Phys Lett* 1998;73(17):2447–9.
- [109] Wang X, Li Q, Xie J, Jin Z, Wang J, Li Y, et al. Fabrication of ultralong and electrically uniform single-walled carbon nanotubes on clean substrates. *Nano Lett* 2009;9(9):3137–41.
- [110] Giordani S, Bergin SD, Nicolosi V, Lebedkin S, Kappes MM, Blau WJ, et al. Debundling of single-walled nanotubes by dilution: observation of large populations of individual nanotubes in amide solvent dispersions. *J Phys Chem B* 2006;110(32):15708–18.
- [111] Furtado CA, Kim UJ, Gutierrez HR, Pan L, Dickey EC, Eklund PC. Debundling and dissolution of single-walled carbon nanotubes in amide solvents. *J Am Chem Soc* 2004;126(19):6095–105.
- [112] Okimoto H, Takenobu T, Yanagi K, Miyata Y, Shimotani H, Kataura H, et al. Tunable carbon nanotube thin-film transistors produced exclusively via inkjet printing. *Adv Mater* 2010;22(36):3981–6.
- [113] Beecher P, Servati P, Rozhin A, Colli A, Scardaci V, Pisana S, et al. Ink-jet printing of carbon nanotube thin film transistors. *J Appl Phys* 2007;102(4):043710.
- [114] Kordas K, Mustonen T, Toth G, Jantunen H, Lajunen M, Soldano C, et al. Inkjet printing of electrically conductive patterns of carbon nanotubes. *Small* 2006;2(8–9):1021–5.
- [115] Mustonen T. Inkjet printing of carbon nanotubes for electronic applications. University of Oulu, Doctoral Thesis; 2009.
- [116] Peng S, Cho K. Ab initio study of doped carbon nanotube sensors. *Nano Lett* 2003;3(4):513–7.
- [117] Maldonado S, Stevenson KJ. Influence of nitrogen doping on oxygen reduction electrocatalysis at carbon nanofiber electrodes. *J Phys Chem B* 2005;109(10):4707–16.
- [118] Lim SH, Elim HI, Gao XY, Wee ATS, Ji W, Lee JY, et al. Electronic and optical properties of nitrogen-doped multiwalled carbon nanotubes. *Phys Rev B* 2006;73(4):045402.
- [119] Kang SJ, Kocabas C, Kim H-S, Cao Q, Meitl MA, Khang D-Y, et al. Printed multilayer superstructures of aligned single-walled carbon nanotubes for electronic applications. *Nano Lett* 2007;7(11):3343–8.
- [120] Meitl MA, Zhou Y, Gaur A, Jeon S, Usrey ML, Strano MS, et al. Solution casting and transfer printing single-walled carbon nanotube films. *Nano Lett* 2004;4(9):1643–7.
- [121] Pandolfo AG, Hollenkamp AF. Carbon properties and their role in supercapacitors. *J Power Sources* 2006;157(1):11–27.
- [122] Zhang J, editor. PEM fuel cell electrocatalysts and catalyst layers. London: Springer, London; 2008.
- [123] Jost K, Perez CR, McDonough JK, Presser V, Heon M, Dion G, et al. Carbon coated textiles for flexible energy storage. *Energ Environ Sci* 2011;4(12):5060–7.
- [124] Jost K, Stenger D, Perez CR, McDonough JK, Lian K, Gogotsi Y, et al. Knitted and screen printed carbon-fiber supercapacitors for applications in wearable electronics. *Energ Environ Sci* 2013;6(9):2698–705.
- [125] Taylor AD, Kim EY, Humes VP, Kizuka J, Thompson LT. Inkjet printing of carbon supported platinum 3-D catalyst layers for use in fuel cells. *J Power Sources* 2007;171(1):101–6.
- [126] Towne S, Viswanathan V, Holbery J, Rieke P. Fabrication of polymer electrolyte membrane fuel cell MEAs utilizing inkjet print technology. *J Power Sources* 2007;171(2):575–84.
- [127] Jeyabharathi C, Venkateshkumar P, Rao MS, Mathiyarasu J, Phani KLN. Nitrogen-doped carbon black as methanol tolerant electrocatalyst for oxygen reduction reaction in direct methanol fuel cells. *Electrochim Acta* 2012;74:171–5.
- [128] Liu J, Sun X, Song P, Zhang Y, Xing W, Xu W. High-performance oxygen reduction electrocatalysts based on cheap carbon black, nitrogen, and trace iron. *Adv Mater* 2013;25(47):6879–83.
- [129] Saha MS, Paul D, Malevich D, Peppley B, Karan K. Preparation of ultra-thin catalyst layers by piezo-electric printer for PEMFCs applications. *ECS Trans* 2009;25(1):2049–59.
- [130] Saha MS, Malevich D, Halliop E, Pharoah JG, Peppley BA, Karan K. Electrochemical activity and catalyst utilization of low Pt and thickness controlled membrane electrode assemblies. *J Electrochem Soc* 2011;158(5):B562–7.
- [131] Malevich D, Saha MS, Halliop E, Peppley BA, Pharoah JG, Karan K. Performance characteristics of PEFCs with patterned electrodes prepared by piezo-electric printing. *ECS Trans* 2013;50(2):423–7.
- [132] Shukla S, Domican K, Secanell M. Effect of electrode patterning on PEM fuel cell performance using ink-jet printing method. *ECS Trans* 2014;64(3):341–52.
- [133] Wang Z, Nagao Y. Effects of Nafion impregnation using inkjet printing for membrane electrode assemblies in polymer electrolyte membrane fuel cells. *Electrochim Acta* 2014;129:343–7.
- [134] Bonifácio RN, Paschoal JOA, Linardi M, Cuenca R. Catalyst layer optimization by surface tension control during ink formulation of membrane electrode assemblies in proton exchange membrane fuel cell. *J Power Sources* 2011;196(10):4680–5.
- [135] Hasché F, Fellingner T-P, Oezaslan M, Paraknowitsch JP, Antonietti M, Strasser P. Mesoporous nitrogen doped carbon

- supported platinum PEM fuel cell electrocatalyst made from ionic liquids. *ChemCatChem* 2012;4(4):479–83.
- [136] Rich SS, Burk JJ, Kong CS, Cooper CD, Morse DE, Buratto SK. Nitrogen functionalized carbon black: a support for Pt nanoparticle catalysts with narrow size dispersion and high surface area. *Carbon* 2015;81:115–23.
- [137] Chen S, Bi J, Zhao Y, Yang L, Zhang C, Ma Y, et al. Nitrogen-Doped Carbon Nanocages as Efficient Metal-Free Electrocatalysts for Oxygen Reduction Reaction. *Adv Mater* 2012;24(41):5593–7.
- [138] Hoth CN, Choulis SA, Schilinsky P, Brabec CJ. On the effect of poly(3-hexylthiophene) regioregularity on inkjet printed organic solar cells. *J Mater Chem* 2009;19(30):5398–404.
- [139] Lee JK, Lee UJ, Kim M-K, Lee SH, Kang K-T. Direct writing of semiconducting polythiophene and fullerene derivatives composite from bulk heterojunction solar cell by inkjet printing. *Thin Solid Films* 2011;519(16):5649–53.
- [140] Lange A, Wegener M, Boeffel C, Fischer B, Wedel A, Neher D. A new approach to the solvent system for inkjet-printed P3HT:PCBM solar cells and its use in devices with printed passive and active layers. *Sol Energy Mater Sol Cells* 2010;94(10):1816–21.
- [141] Dua V, Surwade SP, Ammu S, Agnihotra SR, Jain S, Roberts KE, et al. All-organic vapor sensor using inkjet-printed reduced graphene oxide. *Angew Chem Int Ed* 2010;49(12):2154–7.
- [142] Lu T, Zhang Y, Li H, Pan L, Li Y, Sun Z. Electrochemical behaviors of graphene–ZnO and graphene–SnO₂ composite films for supercapacitors. *Electrochim Acta* 2010;55(13):4170–3.
- [143] Baker J, Deganello D, Gethin DT, Watson TM. Flexographic printing of graphene nanoplatelet ink to replace platinum as counter electrode catalyst in flexible dye sensitised solar cell. *Mater Res Innovations* 2014;18(2):86–90.
- [144] Sinar D, Knopf GK. Printed graphene interdigitated capacitive sensors on flexible polyimide substrates. In: *IEEE 14th International Conference on Nanotechnology*; 2014, p. 538–42.
- [145] Karuwan C, Sriprachubwong C, Wisitsoraat A, Phokharatkul D, Sritongkham P, Tuantranont A. Inkjet-printed graphene-poly(3,4-ethylenedioxythiophene):poly(styrene-sulfonate) modified on screen printed carbon electrode for electrochemical sensing of salbutamol. *Sens Actuat B* 2012;161(1):549–55.
- [146] Huang L, Huang Y, Liang J, Wan X, Chen Y. Graphene-based conducting inks for direct inkjet printing of flexible conductive patterns and their applications in electric circuits and chemical sensors. *Nano Res* 2011;4(7):675–84.
- [147] Mei Q, Zhang Z. Photoluminescent graphene oxide ink to print sensors onto microporous membranes for versatile visualization bioassays. *Angew Chem Int Ed* 2012;51(23):5602–6.
- [148] Sinar D, Knopf GK, Nikumb S. Graphene-based inkjet printing of flexible bioelectronic circuits and sensors. In: *Proceedings of SPIE: Micromachining and Microfabrication Process Technology XVIII*, vol. 8612, 2013, p. 861204.
- [149] Giardi R, Porro S, Chiolerio A, Celasco E, Sangermano M. Inkjet printed acrylic formulations based on UV-reduced graphene oxide nanocomposites. *J Mater Sci* 2013;48(3):1249–55.
- [150] Le LT, Ervin MH, Qiu H, Fuchs BE, Lee WY. Graphene supercapacitor electrodes fabricated by inkjet printing and thermal reduction of graphene oxide. *Electrochem Commun* 2011;13(4):355–8.
- [151] Geng H-Z, Kim KK, So KP, Lee YS, Chang Y, Lee YH. Effect of acid treatment on carbon nanotube-based flexible transparent conducting films. *J Am Chem Soc* 2007;129(25):7758–9.
- [152] Hu L, Wu H, Cui Y. Printed energy storage devices by integration of electrodes and separators into single sheets of paper. *Appl Phys Lett* 2010;96(18):183502.
- [153] Small WR, in het Panhuis M. Inkjet printing of transparent, electrically conducting single-walled carbon–nanotube composites. *Small* 2007;3(9):1500–3.
- [154] in het Panhuis M, Heurtematte A, Small WR, Paunov VN. Inkjet printed water sensitive transparent films from natural gum-carbon nanotube composites. *Soft Matter* 2007;3(7):840–3.
- [155] Denneulin A, Bras J, Carcone F, Neuman C, Blayo A. Impact of ink formulation on carbon nanotube network organization within inkjet printed conductive films. *Carbon* 2011;49(8):2603–14.
- [156] Du HY, Wang CH, Hsu HC, Chang ST, Chen US, Yen SC, et al. Controlled platinum nanoparticles uniformly dispersed on nitrogen-doped carbon nanotubes for methanol oxidation. *Diamond Relat Mater* 2008;17(4–5):535–41.
- [157] Kossyrev P. Carbon black supercapacitors employing thin electrodes. *J Power Sources* 2012;201:347–52.
- [158] Alexander D, Gartner J. *Electric vehicle batteries*. Boulder, CO: Navgant Research; 2014.
- [159] Brodd RJ, Huang W, Akridge JR. Polymer battery R&D in the U.S. *Macromol Symp* 2000;159(1):229–46.
- [160] Dahn JR, Zheng T, Liu Y, Xue JS. Mechanisms for lithium insertion in carbonaceous materials. *Science* 1995;270(5236):590–3.
- [161] Gerouki A, Goldner MA, Goldner RB, Haas TE, Liu TY, Slaven S. Density of states calculations of small diameter single graphene sheets. *J Electrochem Soc* 1996;143(11):L262–3.
- [162] Park M-S, Hyun S-H, Nam S-C, Cho SB. Performance evaluation of printed LiCoO₂ cathodes with PVDF-HFP gel electrolyte for lithium ion microbatteries. *Electrochim Acta* 2008;53(17):5523–7.
- [163] Kim H, Auyeung RY, Piqué A. Laser-printed thick-film electrodes for solid-state rechargeable Li-ion microbatteries. *J Power Sources* 2007;165(1):413–9.
- [164] Hu Y, Sun X. Flexible rechargeable lithium ion batteries: advances and challenges in materials and process technologies. *J Mater Chem A* 2014;2(28):10712–38.
- [165] Wang X, Lu X, Liu B, Chen D, Tong Y, Shen G. Flexible energy-storage devices: design consideration and recent progress. *Adv Mater* 2014;26(28):4763–82.
- [166] Wei D, Andrew P, Yang H, Jiang Y, Li F, Shan C, et al. Flexible solid state lithium batteries based on graphene inks. *J Mater Chem* 2011;21(26):9762.
- [167] Hallinan DT, Balsara NP. Polymer electrolytes. *Annu Rev Mater Res* 2013;43(1):503–25.
- [168] Boukamp BA, Lesh GC, Huggins RA. All-solid lithium electrodes with mixed-conductor matrix. *J Electrochem Soc* 1981;128(4):725–9.
- [169] Fan J, Wang T, Yu C, Tu B, Jiang Z, Zhao D. Ordered, nanostructured tin-based oxides/carbon composite as the negative-electrode material for lithium-ion batteries. *Adv Mater* 2004;16(16):1432–6.
- [170] Lee JK, Smith KB, Hayner CM, Kung HH. Silicon nanoparticles–graphene paper composites for Li ion battery anodes. *Chem Commun* 2010;46(12):2025–7.
- [171] Yao J, Shen X, Wang B, Liu H, Wang G. In situ chemical synthesis of SnO₂–graphene nanocomposite as anode materials for lithium-ion batteries. *Electrochem Commun* 2009;11(10):1849–52.
- [172] Wang D, Yang J, Li X, Geng D, Li R, Cai M, et al. Layer by layer assembly of sandwiched graphene/SnO₂ nanorod/carbon nanostructures with ultrahigh lithium ion storage properties. *Energ Environ Sci* 2013;6(10):2900–6.

- [173] Johnson BA, White RE. Characterization of commercially available lithium-ion batteries. *J Power Sources* 1998;70(1):48–54.
- [174] Wang K, Luo S, Wu Y, He X, Zhao F, Wang J, et al. Super-aligned carbon nanotube films as current collectors for lightweight and flexible lithium ion batteries. *Adv Funct Mater* 2013;23(7):846–53.
- [175] Kiebele A, Gruner G. Carbon nanotube based battery architecture. *Appl Phys Lett* 2007;91(14):144104.
- [176] Ho CC, Evans JW, Wright PK. Direct write dispenser printing of a zinc microbattery with an ionic liquid gel electrolyte. *J Micromech Microeng* 2010;20(10):104009.
- [177] Gaikwad AM, Whiting GL, Steingart DA, Arias AC. Highly flexible, printed alkaline batteries based on mesh-embedded electrodes. *Adv Mater* 2011;23(29):3251–5.
- [178] Song JY, Wang YY, Wan CC. Review of gel-type polymer electrolytes for lithium-ion batteries. *J Power Sources* 1999;77(2):183–97.
- [179] Xu K. Nonaqueous liquid electrolytes for lithium-based rechargeable batteries. *Chem Rev* 2004;104(10):4303–418.
- [180] Hofmann A, Schulz M, Hanemann T. Gel electrolytes based on ionic liquids for advanced lithium polymer batteries. *Electrochim Acta* 2013;89:823–31.
- [181] Rao M, Geng X, Liao Y, Hu S, Li W. Preparation and performance of gel polymer electrolyte based on electrospun polymer membrane and ionic liquid for lithium ion battery. *J Membr Sci* 2012;399–400:37–42.
- [182] Kil EH, Choi KH, Ha HJ, Xu S, Rogers JA, Kim MR, et al. Imprintable, bendable, and shape-conformable polymer electrolytes for versatile-shaped lithium-ion batteries. *Adv Mater* 2013;25(10):1395–400.
- [183] Teran AA, Tang MH, Mullin SA, Balsara NP. Effect of molecular weight on conductivity of polymer electrolytes. *Solid State Ionics* 2011;203(1):18–21.
- [184] Mullin SA, Stone GM, Panday A, Balsara NP. Salt diffusion coefficients in block copolymer electrolytes. *J Electrochem Soc* 2011;158(6):A619.
- [185] Ha H-J, Kil E-H, Kwon YH, Kim JY, Lee CK, Lee S-Y. UV-curable semi-interpenetrating polymer network-integrated, highly bendable plastic crystal composite electrolytes for shape-conformable all-solid-state lithium ion batteries. *Energy Environ Sci* 2012;5(4):6491.
- [186] Baggetto L, Niessen RAH, Roozeboom F, Notten PHL. High energy density all-solid-state batteries: a challenging concept towards 3D integration. *Adv Funct Mater* 2008;18(7):1057–66.
- [187] Kötz R, Hahn M, Gally R. Temperature behavior and impedance fundamentals of supercapacitors. *J Power Sources* 2006;154(2):550–5.
- [188] Vangari M, Pryor T, Jiang L. Supercapacitors: review of materials and fabrication methods. *J Energy Eng* 2012;139(2):72–9.
- [189] Conte M. Supercapacitors technical requirements for new applications. *Fuel Cells* 2010;10(5):806–18.
- [190] Zhang LL, Zhou R, Zhao XS. Graphene-based materials as supercapacitor electrodes. *J Mater Chem* 2010;20(29):5983–92.
- [191] Qu D, Shi H. Studies of activated carbons used in double-layer capacitors. *J Power Sources* 1998;74(1):99–107.
- [192] Wang Y, Shi Z, Huang Y, Ma Y, Wang C, Chen M, et al. Supercapacitor devices based on graphene materials. *J Phys Chem C*. 2009;113(30):13103–7.
- [193] Liu C, Yu Z, Neff D, Zhamu A, Jang BZ. Graphene-based supercapacitor with an ultrahigh energy density. *Nano Lett* 2010;10(12):4863–8.
- [194] Guo CX, Li CM. A self-assembled hierarchical nanostructure comprising carbon spheres and graphene nanosheets for enhanced supercapacitor performance. *Energy Environ Sci* 2011;4(11):4504–7.
- [195] Zhang K, Zhang LL, Zhao XS, Wu J. Graphene/polyaniline nanofiber composites as supercapacitor electrodes. *Chem Mater* 2010;22(4):1392–401.
- [196] Cao X, Shi Y, Shi W, Lu G, Huang X, Yan Q, et al. Preparation of novel 3D graphene networks for supercapacitor applications. *Small* 2011;7(22):3163–8.
- [197] Lu W, Dai L. Carbon nanotube supercapacitors. In: Marulanda JM, editor. *Carbon Nanotubes*. Rijeka, Croatia: InTech; 2010.
- [198] An KH, Kim WS, Park YS, Choi YC, Lee SM, Chung DC, et al. Supercapacitors using single-walled carbon nanotube electrodes. *Adv Mater* 2001;13(7):497–500.
- [199] Xiao Q, Zhou X. The study of multiwalled carbon nanotube deposited with conducting polymer for supercapacitor. *Electrochim Acta* 2003;48(5):575–80.
- [200] Futaba DN, Hata K, Yamada T, Hiraoka T, Hayamizu Y, Kakudate Y, et al. Shape-engineerable and highly densely packed single-walled carbon nanotubes and their application as super-capacitor electrodes. *Nat Mater* 2006;5(12):987–94.
- [201] Lin Y, Watson KA, Kim JW, Baggett DW, Working DC, Connell JW. Bulk preparation of holey graphene via controlled catalytic oxidation. *Nanoscale* 2013;5(17):7814–24.
- [202] Peng Y-Y, Liu Y-M, Chang J-K, Wu C-H, Ger M-D, Pu N-W, et al. A facile approach to produce holey graphene and its application in supercapacitors. *Carbon* 2015;81:347–56.
- [203] Wilson MS, Gottesfeld S. High performance catalyzed membranes of ultra-low Pt loadings for polymer electrolyte fuel cells. *J Electrochem Soc* 1992;139(2):L28–30.
- [204] Wilson MS, Gottesfeld S. Thin-film catalyst layers for polymer electrolyte fuel cell electrodes. *J Appl Electrochem* 1992;22(1):1–7.
- [205] Kocha SS, Zack JW, Alia SM, Neyerlin KC, Pivovarov BS. Influence of ink composition on the electrochemical properties of Pt/C electrocatalysts. *ECS Trans* 2013;50(2):1475–85.
- [206] Hwang DS, Park CH, Yi SC, Lee YM. Optimal catalyst layer structure of polymer electrolyte membrane fuel cell. *Int J Hydrogen Energy* 2011;36(16):9876–85.
- [207] Lee H-K, Park J-H, Kim D-Y, Lee T-H. A study on the characteristics of the diffusion layer thickness and porosity of the PEMFC. *J Power Sources* 2004;131(1–2):200–6.
- [208] Meng X, Yang X-Q, Sun X. Emerging applications of atomic layer deposition for lithium-ion battery studies. *Adv Mater* 2012;24(27):3589–615.
- [209] Jian L, Xueliang S. Elegant design of electrode and electrode/electrolyte interface in lithium-ion batteries by atomic layer deposition. *Nanotechnology* 2015;26(2):024001.
- [210] Perez R, Perez M. A fundamental look at energy reserves for the planet. *IEA/SHC Solar Update*; 2009. 1–3.
- [211] Huang X, Han S, Huang W, Liu X. Enhancing solar cell efficiency: the search for luminescent materials as spectral converters. *Chem Soc Rev* 2013;42(1):173–201.
- [212] Nelson J. Polymer:fullerene bulk heterojunction solar cells. *Mater Today* 2011;14(10):462–70.
- [213] Nielsen TD, Cruickshank C, Foged S, Thorsen J, Krebs FC. Business, market and intellectual property analysis of polymer solar cells. *Sol Energy Mater Sol Cells* 2010;94(10):1553–71.
- [214] Dang MT, Hirsch L, Wantz G. P3HT:PCBM, best seller in polymer photovoltaic research. *Adv Mater* 2011;23(31):3597–602.
- [215] Jørgensen M, Hagemann O, Alstrup J, Krebs FC, Jørgensen M, Hagemann O, et al. Thermo-cleavable solvents for printing conjugated polymers: application in polymer solar cells. *Sol Energy Mat Sol Cells* 2009;93(4):413–21.

- [216] Chen Z, Cotterell B, Wang W, Guenther E, Chua S-J. A mechanical assessment of flexible optoelectronic devices. *Thin Solid Films* 2001;394(1–2):201–5.
- [217] Schlattmann AR, Floet DW, Hilberer A, Garten F, Smulders PJM, Klapwijk TM, et al. Indium contamination from the indium–tin–oxide electrode in polymer light-emitting diodes. *Appl Phys Lett* 1996;69(12):1764–6.
- [218] Suzuki K, Yamaguchi M, Kumagai M, Yanagida S. Application of carbon nanotubes to counter electrodes of dye-sensitized solar cells. *Chem Lett* 2003;32(1):28–9.
- [219] Zhang DW, Li XD, Chen S, Tao F, Sun Z, Yin XJ, et al. Fabrication of double-walled carbon nanotube counter electrodes for dye-sensitized solar cells. *J Solid State Electrochem* 2010;14(9):1541–6.
- [220] Yue G, Wang L, Zhang Xa, Wu J, Jiang Q, Zhang W, et al. Fabrication of high performance multi-walled carbon nanotubes/polypyrrole counter electrode for dye-sensitized solar cells. *Energy* 2014;67:460–7.
- [221] Angmo D, Larsen-Olsen TT, Jørgensen M, Søndergaard RR, Krebs FC. Roll-to-roll inkjet printing and photonic sintering of electrodes for ITO free polymer solar cell modules and facile product integration. *Adv Energy Mater* 2013;3(2):172–5.
- [222] Angmo D, Gevorgyan SA, Larsen-Olsen TT, Søndergaard RR, Hösel M, Jørgensen M, et al. Scalability and stability of very thin, roll-to-roll processed, large area, indium–tin–oxide free polymer solar cell modules. *Org Electron* 2013;14(3):984–94.
- [223] Jang Y, Hartarto Tambunan I, Tak H, Dat Nguyen V, Kang T, Byun D. Non-contact printing of high aspect ratio Ag electrodes for polycrystalline silicone solar cell with electrohydrodynamic jet printing. *Appl Phys Lett* 2013;102(12):123901.
- [224] Hösel M, Søndergaard RR, Angmo D, Krebs FC. Comparison of fast roll-to-roll flexographic, inkjet, flatbed, and rotary screen printing of metal back electrodes for polymer solar cells. *Adv Eng Mater* 2013;15(10):995–1001.
- [225] Todorov TK, Gunawan O, Gokmen T, Mitzi DB. Solution-processed Cu(In, Ga)(S, Se)₂ absorber yielding a 15.2% efficient solar cell. *Prog Photovoltaics* 2013;21(1):82–7.
- [226] Hösel M, Søndergaard RR, Jørgensen M, Krebs FC. Fast inline roll-to-roll printing for indium–tin–oxide-free polymer solar cells using automatic registration. *Energy Technol* 2013;1(1):102–7.
- [227] Chen X, Jia B, Zhang Y, Gu M. Exceeding the limit of plasmonic light trapping in textured screen-printed solar cells using Al nanoparticles and wrinkle-like graphene sheets. *Light Sci Appl* 2013;2:e92.
- [228] Wang DH, Kim JK, Seo JH, Park I, Hong BH, Park JH, et al. Transferable graphene oxide by stamping nanotechnology: electron-transport layer for efficient bulk-heterojunction solar cells. *Angew Chem Int Ed* 2013;52(10):2874–80.
- [229] Li S-S, Tu K-H, Lin C-C, Chen C-W, Chhowalla M. Solution-processable graphene oxide as an efficient hole transport layer in polymer solar cells. *ACS Nano* 2010;4(6):3169–74.
- [230] Lee Y-Y, Tu K-H, Yu C-C, Li S-S, Hwang J-Y, Lin C-C, et al. Top laminated graphene electrode in a semitransparent polymer solar cell by simultaneous thermal annealing/releasing method. *ACS Nano* 2011;5(8):6564–70.
- [231] Choi Y-Y, Kang SJ, Kim H-K, Choi WM, Na S-I. Multilayer graphene films as transparent electrodes for organic photovoltaic devices. *Sol Energy Mater Sol Cells* 2012;96:281–5.
- [232] Andersen TR, Dam HF, Hosel M, Helgesen M, Carle JE, Larsen-Olsen TT, et al. Scalable, ambient atmosphere roll-to-roll manufacture of encapsulated large area, flexible organic tandem solar cell modules. *Energ Environ Sci* 2014;7(9):2925–33.
- [233] Machui F, Hosel M, Li N, Spyropoulos GD, Ameri T, Søndergaard RR, et al. Cost analysis of roll-to-roll fabricated ITO free single and tandem organic solar modules based on data from manufacture. *Energ Environ Sci* 2014;7(9):2792–802.